Title

The water dimer II: Theoretical investigations

Authors

Mukhopadhyay, Anamika
Xantheas, Sotiris S
Saykally, Richard J

Publication Date

2018-05-01

DOI

10.1016/j.cplett.2018.03.057

Peer reviewed

The Water Dimer II: Theoretical Investigations[#]

Anamika Mukhopadhyay,[a] Sotiris S. Xantheas,[b,c,*] and Richard J. Saykally[a,*]

[a] Department of Chemistry, University of California, Berkeley, CA 94720, USA

[b] Advanced Computing, Mathematics and Data Division, Pacific Northwest National Laboratory, 902 Battelle Boulevard, P.O. Box 999, MS K1-83, WA, 99352, USA

[c] Department of Chemistry, University of Washington, Seattle, WA 98195, USA

Abstract

As the archetype of aqueous hydrogen bonding, the water dimer has been extensively studied by both theory and experiment for nearly seven decades. In this article, we present a detailed chronological review of the theoretical advances using electronic structure methods to address the structure, hydrogen bonding and vibrational spectroscopy of the water dimer, as well as the role of its potential energy surface in the development of classical force fields to describe intermolecular interaction in clusters and the condensed phases of water.

[#] Mukhopadhyay, A., Cole, W. T. S., Saykally, R. J., "The Water Dimer I: Experimental Characterization" *Chem. Phys. Lett.*, **633**, 13-26 (2015)

* Corresponding authors: sotiris.xantheas@pnnl.gov (SSX) and saykally@berkeley.edu (RJS)

1. Introduction

As the central prototype for hydrogen bonding, the water dimer first received attention from quantum chemists in early 1968[1], and has ever since been one of the most studied molecular systems. A detailed review by Scheiner[2] summarizes the work reported for this system before 1994. The quasi-linear hydrogen bonded structure was calculated as a stationary point on the intermolecular Potential Energy Surface (PES). Various electronic structure methods (HF, DFT, MP2, MP4, CCSD(T), CI) were used to obtain both the geometry and IPS of the dimer. The computed geometric parameters were compared with reported experimental results.[3,4,5] High- level electronic structure benchmarks are often used to assess the accuracy of lower scaling methods such as new DFT functionals. One of the main thrusts of the previous theoretical investigations was to estimate the hydrogen bond energy and its decomposition into different components (polarization, exchange, induction and dispersion). The dispersion energy, which contributes significantly to these weak interactions and is typically the most difficult component to compute accurately, was estimated using different methods by several groups. Some groups calculated it explicitly or using the SAPT method; otherwise it was added to the SCF energy with an empirical scaling factor. Vibrational frequencies and intensities of both the inter- and intra-molecular modes were calculated and compared with experimental results. These comparisons suggested that inclusion of anharmonic effects in the intermolecular vibrations yielded a good match with experimental transition frequencies. Ab initio calculations correctly reproduce the trend in the experimental spectral shifts and intensity enhancements upon dimerization. Precise far-IR (Thz) high-resolution frequencies and various tunneling splittings were calculated and compared with the Saykally group's experimental data. The water dimer stationary points and PES are of critical importance in the development of transferable, many-body interaction potentials for water. Here we mainly summarize the work published after 1994.

2.Geometry, binding energy and potential energy surface

Morokuma *et al.* reported the first quantum mechanical treatment of the water dimer in 1968.[1] A plethora of theoretical studies have been performed over the last 3 decades to determine its structure, interaction energy and PES. Many of those studies also aimed at benchmarking new, lower-level electronic structure methods for reproducing the results of more accurate methods. Scheiner summarized theoretical studies done up to 1994 in his review.[2] Up to 1994,

the most accurate ab initio equilibrium O···O distance and interaction energy available were 2.949Å and -4.73 kcal/mol, respectively, obtained by van Duijneveldt-van de Rijdt by using counterpoise corrected MP2 and coupled-electron pair theory.[6] Xantheas (1996) converged the O···O distance and the interaction energy to the values of 2.913Å and -5.01kcal/mol, respectively, at the MP2/aug-cc-pV5Z level of theory.[7] Subsequently, a value of -4.98 kcal/mol was obtained for the dimer binding energy by Schütz *et al*. at the MP2 level with ANO-type and uncontracted basis sets in 1997.[8] That value included a BSSE correction of 0.03 to 0.04 kcal/mol and accounted for each monomer's internal structure deformation[7] due to cluster formation. A near linear structure (Figure 1) of C_s symmetry with R_{O-O} distance of 2.925Å was estimated on the counter-poise (CP) corrected CCSD(T) potential energy surface.

The somewhat longer experimental value[3] (2.98 Å) corresponds to the vibrationally averaged value (R_0), as opposed to the results from electronic structure calculations, which usually report the equilibrium (R_e) values. Next year, Schultz et al developed a new variant of the MP2 method, based on localized but orthonormal molecular orbitals, which allowed for BSSE-free geometry optimizations.[9] They showed that the interaction energy for $(H_2O)_2$, calculated using this local electron correlation method without counterpoise corrections, yielded a close agreement with the counterpoise(CP) corrected result, wherein $\delta_{CP} = \Delta E - \Delta E_{CP}$ lies in the range of 0.126 – 0.013 kcal/mol for the different aug-cc-pV*X*Z (*X* = D, T, Q) basis sets. The (uncorrected) interaction energy and equilibrium O···O distance calculated with the LMP2 method using different basis sets (cc-pV*X*Z and aug-cc-pV*X*Z, *X* = D, T, Q) were compared with the full MP2 method results. Energy partitioning showed that ionic interaction played a crucial role, together with dispersion, in stabilizing the dimer. The value of the dimer interaction energy obtained by Famulari *et al.* was -4.69 kcal/mol, which falls in the experimental range of -5.4± 0.7 kcal/mol[5], but appeared lower compared to the value obtained by Schütz *et al*.[8,9].[10] General molecular orbital-valence bond (MO-VB) treatment based on SCF-MI wavefunctions was used for the interaction energy

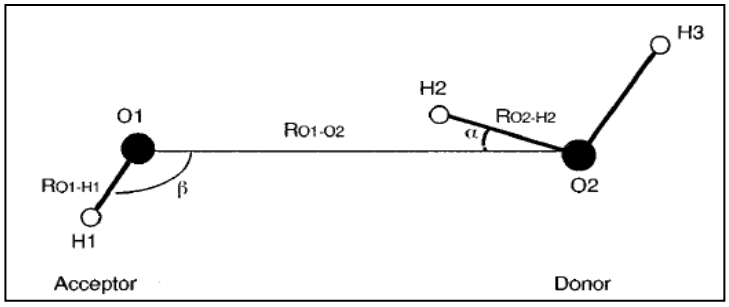

Figure 1. The trans-linear geometry obtained using MP2 method by Schütz *et al*.[8]

calculation. The VB treatment considers effects of orbital overlap between two fragments to describe intermolecular interaction. This method works well for both the long- and short-range parts of the water dimer PES. The equilibrium R_{O-O} distance was calculated to be 3.0 Å by the VB method and appeared longer than the experimental (vibrationally averaged) result[3,4]. In the equilibrium structure of the dimer, the geometry of the acceptor molecule remains practically unchanged, whereas the "hydrogen bonded" O–H bond of the donor molecule is elongated by 0.0002 Å. The effect of temperature on the structure of water dimer was studied by Bandyopadhyay *et al.* in 1999 employing ab initio multicanonical Monte Carlo simulations.[11] The most stable structure was of C_s symmetry with a linear hydrogen bond, as reported by Schütz *et al*.[8]. The other two structures with C_{2v} and C_i symmetry, which are essentially the bifurcated and cyclic structures, were identified as transition states. The authors reported the energy fluctuation $(\langle E^2\rangle-\langle E\rangle^2)/k_BT^2$ over a 250K temperature range (Figure 2), observing a broad peak in the temperature range of 150K – 250K. The energy fluctuation increases with temperature below 150K and decreases with temperature above 200K. This behavior was attributed to the presence of different structures at different temperatures. The angular distribution (θ) study of the O–H···O hydrogen bond indicated that the dimer structure remains linear with a small θ value at temperatures 100, 200, and 280K. However, at 300K and 500K the higher value of θ indicates that the population of bent structures became comparable with that of the linear structure. Finally, these authors concluded that two different stages of structural changes are occurring for the water dimer within the simulated temperature range. The first stage is related to a distorted linear structure in the low temperature range, whereas the second stage is related to a transition from a linear to a bent structure in the high temperature range. Hobza *et al*. (1999) reported the geometry optimization and stabilization energy of water dimer with both standard and counterpoise (CP) corrected PES using MP2 level of theory and different basis sets (6-31G**, cc-pV*X*Z and aug-cc-pV*X*Z, where X = D, T, Q).[12] Their calculations suggested a

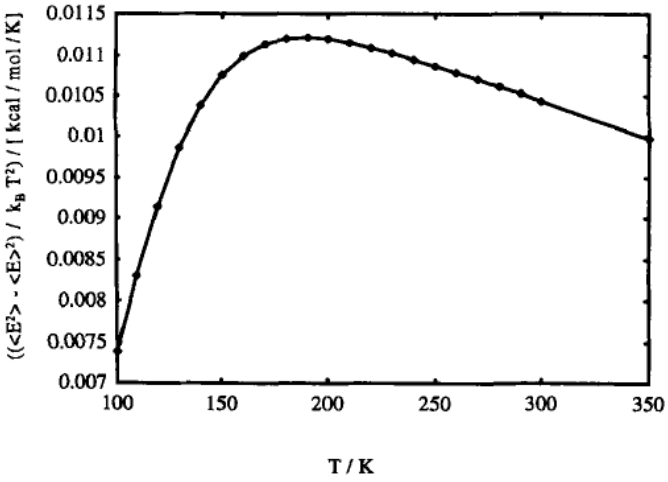

Figure 2. The energy fluctuation plotted as a function of temperature.[11]

smaller variation with basis set on the R_{O-O} distance (~2.91 Å). On the other hand, the R_{O-O} distance was found to be longer on the CP-corrected PES and it converged slowly to 2.9 Å with the larger sets in the aug-cc-pV*X*Z basis set series. The theoretically obtained stabilization energy also yielded best agreement with experiment with the large basis sets. The R_{O-O} distance and interaction energy obtained by Hobza *et al*. yielded good agreement with the values previously reported by Xantheas.[7] Halkier *et al*. (1997) investigated the water dimer equilibrium geometry and interaction energy at the MP2/aug-cc-pVQZ and CCSD(T)/aug-c-pVTZ levels of theory.[13] Their equilibrium O···O distance was reported at 2.90 Å, smaller than the vibrationally averaged experimental value[4] (2.976 Å). Given the fact that the electronic structure level of theory used produces practically converged results for the equilibrium distance, this "difference" accounts for the effect of anharmonicity on the intermolecular distance. The interaction energy was obtained as -5.0±0.1 kcal/mol, which is within the error bar of the experimentally estimated value of -5.4±0.7 kcal/mol[5]. These authors concluded from this study that basis sets with diffuse functions yielded better value for interaction energy. Later, Halkier *et al.* examined the HF and correlation contributions to the interaction energy of $(H_2O)_2$ along with other hydrogen bonded complexes viz. $(HF)_2$, $(HCl)_2$, H_2OHF, HCNHF at different correlation levels [MP2, CCSD(T)] using the aug-cc-pV*X*Z basis set series.[14] The interaction energy at the SCF correlation level converged very unsystematically, irrespective of the incorporation of the CP correction. The CCSD(T) method yielded the most accurate interaction energy (-4.96 kcal/mol) for $(H_2O)_2$, obtained using the combination of ΔE^{ave} results with the ΔE_{corr}^{CP} results. Klopper *et al*. employed the CCSD(T) method with fixed monomer deformation coordinates to evaluate the equilibrium geometry and dissociation energy of the dimer.[15] The values for the equilibrium O···O distance and the equilibrium interaction energy obtained were R_e=291.2±0.5 *pm* (2.912±0.005 Å) and D_e=-21.0±0.2 kJ/mol (-5.02±0.05 kcal/mol). The equilibrium geometry of the dimer obtained from different groups was composed by these authors

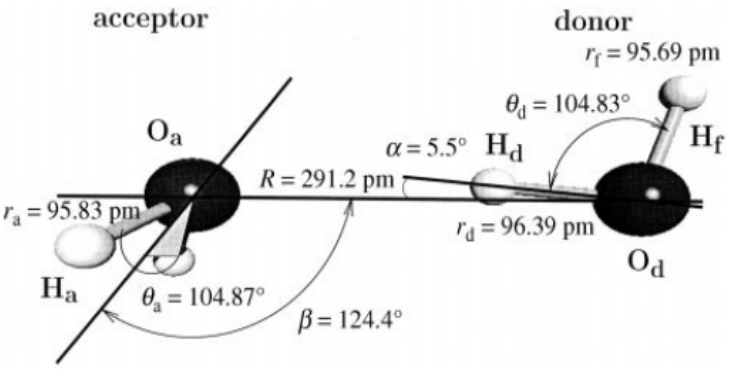

Figure 3. The equilibrium geometry of the water dimer as composed by Klopper *et al.*[15]

in Figure 3.

Grigorenko *et al*. (2000) employed the Diatomics-In-Molecule (DIM) approach to construct the PESs for the$(H_2O)_n$, n=2-6 clusters.[16] The DIM Hamiltonian is $H_{DIM}=H_{intra}+H_{inter}-H_{atomic}$, where the first two terms arise from the intra- and inter-molecular contributions and the last one is the atomic contribution. Both the calculated R_{O-O} distance of 3.0 Å and interaction energy of -5.65 kcal/mol were larger compared to the high level results. In 2000, van der Avoird and co-workers developed a new ab initio potential with a site-site approach termed symmetry adapted perturbation theory (SAPT-5s) using 2510 configurations of the water dimer.[17] The computed R_{O-O} distance of 2.91±0.005 Å was very close to the value obtained by high level electronic structure theory. The depth of SAPT minimum was estimated at D_e=-4.86 kcal/mol. The potential dissociates into two water monomers and the dissociation energy was calculated as D_0=1,165±54 cm^{-1} (3.33±0.15 kcal/mol), consistent with value of D_0=3.23±0.1 kcal/mol previously reported by Feyereisen *et al.*[18]

Torheyden *et al*. (2006) developed an analytical PES based on a model, which considered contributions from electrostatics, first-order exchange, induction plus exchange-induction and dispersion plus exchange-dispersion.[19] All these components of the energy were obtained from SAPT calculations with the aug-cc-pVTZ basis set. The water dimer geometry was calculated by imposing tetrahedral orientation using rigid monomers at their vibrationally averaged geometries. The intermolecular PES was then obtained at different R_{O-O} distances (2.5, 2.75, 3.0, 3.25 and 3.5 Å).

Smith et al (1990) first obtained ten stationary points on the dimer PES at the MP2/6-311+G(*d*,*p*) level of theory.[20] The minimum energy structure was a linear geometry with C_s symmetry, similar to that reported earlier by Schütz *et al.*[8] and Bandyopadhyay *et al*.[11] The search of stationary points by Smith *et al*. was further refined by Tschumper *et al.* (2002) at the CCSD(T)/(TZ2P(*f*,*d*)+dif level of theory.[21] Only the C_s symmetry non-planar open structure was reported as the minimum, in agreement with the previous studies. Among the other nine reported structures, three were determined to be transition states and the rest of them were higher energy saddle points. A full-dimensional ab initio PES was reported by Bowman and co-workers (2006) at the CCSD(T)/aug-cc-pVTZ level of theory as the result of fitting 19,805 dimer configurations.[22] Ten stationary points were identified on that PES. As for Smith and Tschumper, these authors identified the linear geometry (C_s symmetry) as the global minimum on PES. The

dimer PES dissociated in two monomer molecules with a dissociation energy of D_e=1,665.74 cm^{-1} (note that the value of 1,165±54 cm^{-1}previously reported by van der Avoird and coworkers[17] corresponds to D_0). Bowman and co-workers in a subsequent year (2008) evaluated intramolecular vibrational energies of both $(H_2O)_2$ and $(D_2O)_2$ using their full dimensional PES.[23] They further extended their study to develop a new potential energy surface for $(H_2O)_3$. In 2009, Bowman and co-workers introduced three modifications to their full-dimensional $(H_2O)_2$ dimer PES and this modified potential was named HBB2.[24] The corrections consisted the use of (*i*) a modified set of electronic energies to obtain the dissociation energy (D_e), (*ii*) a spectroscopically accurate water monomer potential and (*iii*) a smoothly varying 'hybrid potential' where the HBB2 PES switches to the TTM3-F PES,[25] which accurately describes the long range behavior of the dimer. The use of the modified electronic energies improved the D_e value from -4.75 to -4.98 kcal/mol, which was now in agreement with the high level electronic structure results.[21,13,14] It should be noted that this potential produced a value[24] of D_0 = 1,103 ± 4 cm^{-1}, which was subsequently found (*vide infra*) to be within the experimentally obtained value of 1,110 ± 10 cm^{-1}.[26] Bowman and co-workers summarized the development of their flexible, full-dimensional, *ab initio* based potential in a review.[27] The initial development of the SAPT based dimer PES by van der Avoird and co-workers (2008) was followed by the further development of a six-dimensional interaction potential (CC-pol).[28,29] Similar to their previous effort, they fitted the *ab initio* energies of 2,510 dimer configurations (obtained using rigid monomers) in the vicinity of minima and saddle points. They used the MP2 energies at the complete basis set limit and the contribution from CCSD(T) energies computed with the aug-cc-pV*X*Z (*X* = T, Q) basis sets. They obtained the same number of stationary points (10) as before and the same global minimum structure. Amadei *et al*. in 2002 developed a new Hamiltonian based on a first principles model for polarizable water.[30] This first principles model expands the charge density up to the quadrupole term and the molecular polarizability to linear term and also incorporates a short range atomic repulsion in the Hamiltonian as a semi-empirical function. The binding energy and total dipole moment of the water dimer obtained using this first principles model for different monomer orientations produced a good agreement with the more sophisticated CCSD(T) results. In a subsequent effort in 2008, Amadei and co-workers refined their model and applied it to larger water clusters up to the heptamer.[31] In 2013, the optimized geometry of the water dimer with the CCSDTQ method extrapolated to the complete basis set

(CBS) limit and including CP corrections at the CCSD(T)-F12b/CBS level was reported.[32] The interaction energy/$R_{O\text{-}O}$ distance obtained at the cc-pVTZ-F12/cc-pVQZ-F12 basis set limit was just 0.002 kcal/mol higher/0.0005 Å shorter compared to the aug-cc-pVQZ/aug-cc-pV5Z result. Tschumper and co-workers have recently characterized water dimer through hexamer clusters using the 2-body:Many-body CCSD(T):MP2approach carried out at the CBS limit using basis sets as large as haQZ.[33] They showed that the O–H bond length and the hydrogen bond distance O···H were overestimated by 0.006-0.007Å and 0.01-0.02Å, respectively, by the haDZ compared to the haQZ basis set.

3. Thermodynamic properties

Thermodynamic properties of water dimer, viz. the dimerization constant and population of water dimers in saturated steam, have been investigated by Slanina and co-workers.[34–44] A close agreement with the experimental observation was obtained using the results of high level *ab initio* theory and water dimer potentials improved over time. Within the scope of this paper, we will discuss only the developments after 2000. In 2001, the thermodynamic calculations were performed for the global minimum of the dimer (C_s symmetry) using Rigid Rotor and Harmonic Oscillator partition functions (RRHO), and it was found that the mole fraction of dimer increases with increasing temperature. This behavior was attributed to the subtle balance between the increase in saturated pressure with temperature and the decrease in the equilibrium constant with temperature.[40,41] These authors revised the water dimer thermodynamics within the anharmonic regime during subsequent studies.[42–44] The change in the Gibbs free energy (ΔG^0_2) was evaluated over a temperature range using an anharmonic partition function obtained at the MP2/6-311++G**[42,43] and theMP2/aug-

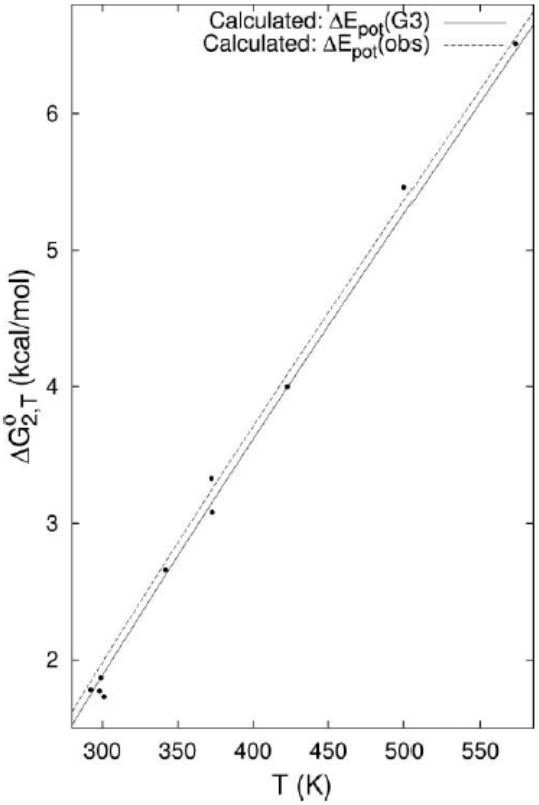

Figure 4. Observed and computed changes in the Gibbs free energy.[43]

cc-pVQZ[44] levels. The result using this anharmonic treatment yielded a better agreement with the observed data, as compared to the harmonic results. The water dimerization energy of -3.103 kcal/mol at T = 0K obtained using this anharmonic approach yielded a very good agreement with the reported spectroscopic value of -3.159 kcal/mol.[26] Note that the previously reported value[18] (-3.23±0.1 kcal/mol) based on scaled harmonic frequencies is just 0.1 kcal/mol larger than this result. As mentioned earlier, theory has already predicted a D_0 value of 1,103 ± 4 cm^{-1} as the result of the benchmark work by Bowman and co-workers with the HBB2 potential[24] and at the time even called for the experimental verification of that number, something that was indeed subsequently confirmed experimentally by the Reisler group, which suggested a value of 1,105 ± 10 cm^{-1} [26]. A comparison with the observed data,[5,26,45–48] as reported by Slanina *et al*.,[44] is shown in Figure 4. These authors have extended their study for a water dimer encapsulated in Fullerene cages. In particular, the encapsulation in C_{60} and in two of the most common C_{84} fullerene cages was investigated[43,44] during geometry optimizations at the M06-2X/6-31G** level of theory. The encapsulation in the cages of the C_{84} fullerene having D_2 and D_{2d} symmetry resulted in shorter dimer $R_{O\text{-}O}$ bond lengths, yielding the values of 2.745 and 2.680 Å, respectively, when compared to the gas phase (non-encapsulated) water dimer.

The thermochemistry of formation of the water dimer and higher clusters was investigated by Dunn *et al*.[49] They employed Gaussian-2, Gaussian-3, Complete Basis Set (CBS)-QB3, and CBS-APNO methods to obtain $\Delta H°$ and $\Delta G°$ values for water clusters. The water dimer concentration in the saturated water vapor at 298 K predicted by this calculation was 9×10^{14} molecules/cm^3, which produced good agreement with the value 6×10^{14} molecules/cm^3 obtained by Pfeilsticker *et al*.[45] at 292.4K.

4. Performance of Density Functional Theory and other lower level methods

Density Functional Theory (DFT) calculations using various functionals have been reported for the water dimer by several groups and the accuracy of these results compared with highly accurate, benchmark *ab initio* calculations as a means of assessing the performance of the various functionals in describing hydrogen bonding. Wu *et al*. in 2001 reported the performance of pure and hybrid DFT methods to estimate the binding energy of the water dimer in its equilibrium geometry and the results were compared with the SAPT and coupled cluster methods.[14,50] The dimer interaction energy, shown in Figure 5, was plotted as a function of the

center of mass separation between two water molecules obtained using the HF method and different density functionals. Both the HF and pure DFT methods were reported to underestimate the water dimer interaction energy. However, the addition of the long range damped dispersion to the B3VWN5 functional makes the dimer interaction energy comparable with the *ab initio* estimated values. Tsuzuki *et al*. compared the value of water dimer binding energy obtained using the PW91 functional with that of BLYP, B3LYP, MP2 and CCSD(T) values. The aug/cc-pV*X*Z (*X* = D, T, Q, 5) basis set series was used with these DFT functionals. Unlike MP2, the PW91 functional doesn't show a significant change in the magnitude of the interaction energy with the increase in basis set size.

The PW91/aug-cc-pVXZ level slightly overestimates the water dimer binding energy compared to the reported experimental value[5]. Misquitta used frequency-dependent density susceptibilities obtained from time-dependent DFT calculations to estimate the dispersion energy for van der Waals and hydrogen bonded dimers.[51] The dispersion energy calculated in such a way was termed Coupled Kohn-Sham (CKS) dispersion energy and was estimated at the equilibrium geometry (C_s symmetry) of a water dimer with a 3.0 Å center of mass separation between the two monomers. The result was compared with a benchmark value of 2.472 kcal/mol obtained at the SAPT/aug-cc-pVQZ level. No significant variation in the water dimer interaction energy was observed with different basis sets (HCTH407, B97-2 and PBE0) for the CKS method. The percentage of error relative to the benchmark value was 5.5% for the CKS method, a significant improvement over the SAPT(KS) approach, which yielded a maximum percentage of error of 50%. Xu and Goddard examined the performance of the extended density functional (X3LYP), which yielded values of -0.216 eV and 2.908 Å for the interaction energy and $R_{O\text{-}O}$ distance.[52] In comparison with the benchmark *ab initio* values obtained at the G2 level of theory[15] an error of 0.002 eV in the binding energy and 0.004 Å in the

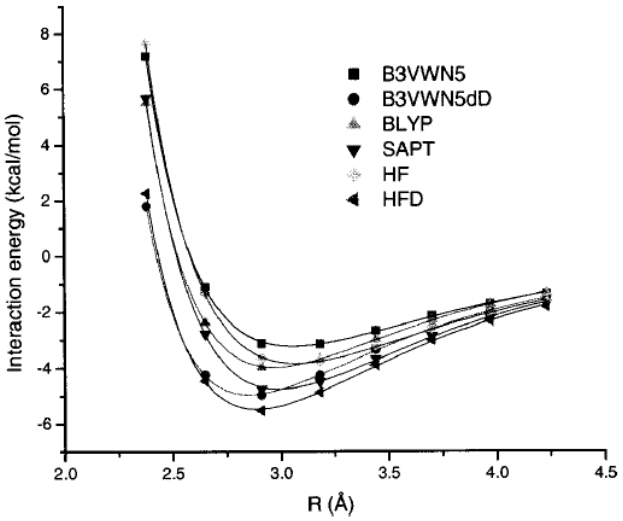

Figure 5. The interaction energy of the water dimer for the equilibrium geometry configuration calculated at different center of mass separations between the two monomers.

O···O distance was reported. These authors subsequently[53] (2004) evaluated various ground state properties (geometry, bond energy, dipole moment, vibrational frequencies etc.) of the water monomer and dimer using a variety of density functionals and compared these results with one another and with those from benchmark *ab initio* calculations[15,21]. They reported results using the LDA(SVWN), seven pure GGA funtionals (B3LYP, BP86, BPW91, PWPW, mPWPW, PBEPBE, XLYP) and eight hybrid GGA funtionals (BH&HLYP, B3LYP, B3P86, B3PW91, PW1PW, mPW1PW, PBE1, PBE, X3LYP). Among all those, the X3LYP functional, which is a linear combination of Becke and Perdew exchange functionals, yielded the best result for the previously mentioned properties and a good agreement was found with the CCSD(T) results. The errors in the estimation of the water dimer binding energy, bond length and vibrational frequencies using the X3LYP functional were 0.05 kcal/mol, 0.004 Å and 12 cm^{-1}, respectively. The good performance of hybrid GGA functionals in yielding water dimer ground state properties prompted Perdew and co-workers (2005) to further test the accuracy of the Perdew-Burke-Ernzerhof (PBE) and the Tao-Perdew-Staroverov-Scuseria (TPSS) functionals to obtain the properties of a test set proposed by Dahlke and Truhlar.[54] This set consisted of non-planar open (C_s), cyclic (C_{2h}), liquid phase (NVT), vapor-phase (vapor at T = 523K) and high pressure (Ice VIII at P = 50GPa) water dimer configurations, with the last three extracted from simulations. They used 11 basis sets [6-31+G(*d*,*p*), 6-31+G(*d*,2*p*), 6-31+G(*d*,3*p*), 6-311+G(*d*,*p*), 6-311+G(*d*,2*p*), 6-311+G(2*d*,2*p*), 6-311+G(2*df*,2*p*), cc-pVTZ, and aug-cc-pV*X*Z with X = D, T, Q] with one variation of PBE functional (PBE1W) in conjunction to the above two functionals. Other than the cyclic (C_{2h}) and the compressed "Ice VIII 50 GPa dimer", the PBE functional with the aug-cc-pVTZ basis set yielded good agreement with the results obtained from high level calculations. The binding energy of the cyclic C_{2h} dimer was underestimated by 0.65 kcal/mol while it was overestimated by 0.59 kcal/mol for the high pressure (P = 50 GPa) compressed dimer with the PBE functional. The modified PBE1W functional removed the under-binding and over-binding effects for the water dimer C_{2h} configuration and the Ice VIII structures. The PBE1W functional in conjunction with the 6-311+G(2*d*,2*p*) basis set yielded the best agreement with the reference. The TPSS functional yielded the best result in combination with the 6-31+G(*d*,*p*) basis set. Among the above-mentioned basis sets, the 6-31+G(*d*,*p*) basis shows an over-binding effect of 1.5 kcal/mol. This over-binding effect improved by the addition of *p* and *d* functions on the hydrogen and oxygen atoms, respectively. On the other hand, inclusion of *f*

functions did not result in further improvement. From the performance of a series of basis sets, they concluded that the addition of diffuse functions on the oxygen and *p* functions on the hydrogen atoms improve both the binding energy and geometric parameters of the water dimer. Glendening performed natural energy decomposition analysis (NEDA) in combination with the DFT method to investigate the dimer hydrogen bond energy.[55] The interaction energy (ΔE) was treated as a summation of the electrical interaction, charge transfer, and core repulsions, wherein the first two components account for the long-range and the latter one accounts for the short-range interaction. The water dimer structure (C_s symmetry) optimized at the B3LYP/aug-cc-pVTZ level was used for the NEDA analysis. It was reported that both the electrical and charge transfer contributions are almost equal (their values were -9.85 and -8.91 kcal/mol, respectively). The major part (~80%) of the charge transfer component originates from the electron transfer from the oxygen lone pair of the donor molecule to the O–H antibonding orbital of the acceptor molecule. Couto *et al*. (2005) reported Monte-Carlo/DFT calculations to obtain the electronic properties of water clusters $(H_2O)_n$, n = 2, 4, 8, 10, 15, 30 with a reparametrized exchange-correlation functional (MPW1PW91).[56] The exchange-correlation functional, modified using an optimal value of the parameter α=0.375, reproduced the first ionization potential (11.21±0.09 eV) of the water dimer. Among various electronic properties, the dipole moment (μ), the interaction energy (ΔE) and the HOMO-LUMO energy difference (E_G) of $(H_2O)_2$ obtained with the above reparametrized exchange-correlation were in very good agreement with the values from high level *ab initio* calculations as well as experiment. On the other hand, the vibrational frequencies were overestimated with this newly parameterized functional. The adiabatic band gap (6.83±0.05 eV) of liquid water estimated from hydration energies for $OH^{\bullet}$ and the adiabatic ionization energy was in excellent agreement with the experiment value. Anderson and Tschumper (2006) reported geometry optimizations and vibrational frequency calculations for ten stationary points using ten density functionals (X3LYP, B3LYP, B971, B98, MPWLYP, PBE1PBE, PBE, MPW1K, B3P86, BHandHLYP) with the TZ2P(*f*,*d*)+dif basis set.[57] The geometries and relative energies of the ten stationary points predicted by these ten functionals produced an overall good agreement with results at the CCSD(T) level. However, all ten functionals, save BHandHLYP, yielded the wrong number of imaginary frequencies for the cyclic structure of C_2 symmetry. Thar *et al*. (2007) compared the performance of plane wave

basis sets with respect to a Gaussian basis for the description of the hydrogen bond with the water dimer as an example.[58]

Shields and Kirschner (2008) also obtained the interaction energies and structures of the water dimer through hexamer and octamer clusters using different DFT functionals.[59] The geometry optimization of the water dimer through the pentamer and the different structural forms of the water hexamer (cage, prism and cyclic) as well as the two cube octamers were reported at the B3LYP/6-31+G(*d*,2*p*) and PBE1W/MG3S DFT levels. A few other higher-lying structures, of the water tetramer and pentamer found on the MP2 PES, were optimized at theX3LYP/aug-cc-pVTZ and B971/6-311++G(3*df*,3*pd*) levels. The interaction energies obtained at the B3LYP/aug-cc-pVTZ level using the B3LYP/6-31G* geometries appear poorer than the results obtained at theB3LYP/6-31+G(*d*,2*p*) level of theory. In addition, the geometry and binding energy of the cyclic, ring-type structures obtained using PBE/MG3S and X3LYP/aug-cc-pVTZ(-*f*) density functional methods yielded a good agreement with the CBS-APNO[49] and the MP2/CBS[7,60] results. However, the above DFT methods failed to describe the pyramidal tetramer or cage type pentamer structures, which are more complex than the cyclic ring structure. This poor performance was attributed to the deficient description of the London dispersion forces in those DFT methods. Mattson *et al*. (2009) compared the results for the water dimer obtained with the AM05 density functional with five other functionals, namely LDA, PBE, PBEsol, RPBE, and BLYP.[61] The water dimer interaction energy of -4.9 kcal/mol obtained using the AM05 functional was in close agreement (within ~0.1 kcal/mol) with the CCSD(T) result, however this DFT method slightly underestimated the $R_{O\text{-}O}$ distance. The PBE functional, on the other hand, was found to slightly over-bind the water dimer and underestimate the $R_{O\text{-}O}$ distance. The RPBE functional under-binds the water dimer by ~1.0 kcal/mol and overestimates the $R_{O\text{-}O}$ distance by 0.01Å. These authors also performed DFT-MD simulations to obtain the properties of liquid water from a 15-50 *ps* simulation of a water cell containing 64 water molecules. Different functionals yielded different structures for liquid water depending on the temperature/rate of thermalization. The RPBE functional at T = 300K produced a liquid state for water, while on the other hand the PBE and AM05 functionals yielded a glassy state at the same temperature. That led the authors to conclude that the good prediction of the binding energies of small water clusters with a given functional represents a necessary, but not sufficient condition for accurately predicting the structure of liquid water with that functional.

Santra *et al*. (2009) assessed the performance of three exchange correlation (XC) density functionals (B3LYP, PBE and PBE0) during simulations of liquid water.[62] They considered a cubic box of length 9.8528 Å containing 32 D_2O molecules and ran a 30 *ps* Born-Oppenheimer Molecular Dynamics simulation. They extracted water monomer and dimer configurations from the liquid water simulations. A total of 66 water dimer structures were selected from the first coordination shell within the R_{O-O} distance ≤3.4 Å. Among the three XC functionals, PBE0 yielded the best agreement with the CCSD(T) results for the dissociation energies of deformed dimers. The average error with the PBE0 functional was 1.0 meV, whereas the average errors with the B3LYP and PBE functionals were 43 and 80 meV, respectively. These large errors were attributed by the authors to the underestimation of the monomer deformation energy.

Head-Gordon and co-workers (2009) have rationalized the contribution of the charge transfer (CT) interaction to the total hydrogen bond energy for the water dimer.[63] They used the Energy Decomposition Analysis (EDA) and the Charge-Transfer Analysis (CTA) techniques, developed by Head-Gordon's group, which are based on the Absolutely Localized Molecular Orbitals (ALMOs). The EDA for the water dimer was performed at the B3LYP/aug-cc-pV*X*Z (*X*=D, T, Q, 5) level of theory using the dimer geometry obtained at the MP2/aug-cc-pVQZ level of theory. The energy and charge transfer components showed a rapid convergence with increasing basis set size. Their analysis showed that all the energy components (frozen density, polarization and charge transfer) share almost equal importance in stabilizing water dimer in its ground state equilibrium geometry. The authors showed that CT contributes 35% of the total hydrogen bond energy and the value is 2.3 meV, which is much smaller than that obtained from Mulliken, Löwdin, and Natural Population Analysis (NPA) methods.

Plumley and Dannenberg (2010) choose the water dimer as a model system to test the performance of ten density functional methods (B3LYP, M05, M05-2X, M06, M06-2X, B2PLYP, B2PLYPD, X3LYP, B97D, and MPWB1K) in combination with 16 basis sets (6-31G(*d*), 6-31G(*d*,*p*), 6-31++1G(*d*,*p*), 6-311G(*d*,*p*), 6-311++G(*d*,*p*), 6-311++G(3*df*,2*p*), D95(*d*,*p*), D9511(*d*,*p*), cc-pV*X*Z and aug-cc-pV*X*Z (*X*= D, T, Q, 5).[64] The purpose of that study was to find a cost effective combination of functional/basis set, which yields the H-bond interaction energy (Δ*E*) and the water dimer geometry in close agreement with high level *ab initio* results. Counterpoise (CP) correction was found to improve the results for the smaller basis sets, which otherwise yield inaccurate geometries and larger interaction energies. On the other hand, the

larger basis sets, as expected, minimized the difference in the interaction energy between the CP corrected and un-corrected geometry. As an example, for aug-cc-pV5Z set this difference was 0.005 kcal/mol for MPWB1K, 0.008 kcal/mol for B3LYP and 0.207 kcal/mol for X3LYP functionals. Among the smaller basis sets, D95(*d*,*p*) provided accurate geometries with almost all the functionals considered in that study.

Huš and Urbic (2012) reported the effect of local environment on the strength of the water dimer hydrogen bond using the B3LYP density functional method in combination with 6-31++G(*d*,*f*) and aug-cc-pVTZ basis sets.[65] Among different possible orientations of two water molecules, the equilibrium dimer geometry was chosen via the B3LYP/6-31++G(*d*,*f*) method, wherein the interaction energy is -6.147 kcal/mol at the O···O distance of 2.892 Å. The local environment was defined as that wherein each of the two monomers can interact with another three water molecules. The authors added six water molecules in the first solvation shell of a dimer molecule and computed the corresponding change (increase or decrease) in the dimer hydrogen bond strength. For the addition of each water molecule, the former changes by 0.73 kcal/mol for B3LYP/6-31++G(*d*,f) and by 0.78 kcal/mol for B3LYP/aug-cc-pVTZ. This number is consistent with the MP2/aug-cc-pVTZ result, wherein a 0.65 kcal/mol change in energy was observed per water molecule. The decrease in the HB strength was observed when an additional molecule was introduced as an acceptor in the environment of a donor or as a donor in the environment of an acceptor. Conversely, an increase was observed for the opposite introduction, i.e. a donor molecule in a donor environment and an acceptor one in an acceptor environment. The hydrogen bond length also changes in a linear additive fashion (increasing or decreasing) by 0.028Å for B3LYP/6-31++G(*d*,*f*) method and by 0.040Å for B3LYP/aug-cc-pVTZ. Furthermore, the addition of water molecules in the second coordination shell changes the HB strength by a third of the value estimated for each water in the first coordination shell.

5. Vibrational energy and anharmonic frequencies

There exist several calculations of the vibrational frequencies and intensities for the water dimer employing quantum mechanical methods. Jung *et al*. (1996) used the Vibrational Self-Consistent Field (VSCF) and the MP2/VSCF method to obtain the frequencies and intensities of the intra- and inter-molecular modes of the water dimer through pentamer clusters.[66] Bowman and co-workers have reported intramolecular fundamentals of the dimer using an accurate

potential energy surface via VSCF/CI calculations using MULTIMODE[23,24]. The 12 dimer vibrational modes (6 intra- plus 6 inter-molecular) were categorized as stiff, intermediate and soft modes depending on the spectral shift and coupling between them. A large anharmonic blue shift with an accompanied significant change in intensity was observed for soft modes, like shearing and torsion. A red shift and a small change in intensity were observed for most of the stiff and intermediate modes. Kjaergaard and co-workers (1999) calculated the IR vibrational frequencies and intensities of the water dimer and trimer using the Harmonically Coupled Anharmonic Oscillator (HCAO) local mode model and an *ab initio* dipole moment function.[67] The level of calculation used was HF and QCISD in combination with the 6-31G(*d*), 6-311+G(*d*,*p*) and 6-311++G(2*d*,2*p*) basis sets. The hydrogen bonded O–H stretching fundamental vibration was red shifted and its intensity was the highest among other O–H stretching modes. On the other hand, the calculated symmetric stretching vibration was the weakest among all four fundamental O–H stretching vibrations and was not observed experimentally. The overtone transitions ($\Delta\nu_{OH} \geq 3$) exhibit more local mode behavior and their intensity decreases with increasing basis set size. In 2003, Schofield and Kjaergaard used their previous HCAO model to obtain the O–H stretching and HOH bending frequencies and intensities of the water dimer, where the coupling between the O–H stretching and HOH bending modes was considered.[68] The PES was calculated at the QCISD/6-311++G(2*d*,2*p*) level of theory. The bonded O–H stretching fundamental was red-shifted compared to the water monomer O–H stretch. On the other hand, the HOH bending fundamental of the donor monomer was blue-shifted compared to monomer bending. Three vibrations in the O–H stretching fundamental region were observed as before. One HOH bending fundamental near 1,600.6 cm^{-1} was assigned to the acceptor unit. The three other bands at 1,613.8, 1,614.7 and 1,628.6 cm^{-1} were assigned as the complex rotational structure of the donor bending mode. In 2007, Kjaergaard and co-workers estimated the bonded O–H stretching vibration at the CCSD(T)/aug-cc-pV*X*Z (*X* = D, T, Q) level of theory.[69] The estimated band appearing at 7,047 cm^{-1} was assigned to the first overtone of the stretching vibration, although this very weak transition was not actually observed experimentally. Subsequently, Kjaergaard *et al*. (2008) extended their calculation in the overtone region up to 8,000 cm^{-1} using different perturbation theory and *ab initio* models (VPT2, VSCF, cc-VSCF and HCAO) in conjunction with the CCSD(T)/aug-cc-pVTZ level of theory.[70] The HCAO model estimated the O–H stretching bands accurately, however this was not the case for the bending

mode. Among all these methods, the VPT2 model worked well for all frequencies except the high-energy vibrations. Kjaergaard and co-workers calculated both the free and hydrogen bonded O–H stretching fundamentals and the overtone band profiles using the local mode Hamiltonian approximation.[71] This model Hamiltonian includes adiabatically separated low energy O···O and high energy O–H stretching modes. The CCSD(T)/aug-cc-pVTZ level of theory was employed to obtain the optimized geometry. Transitions between different possible O···O stretching modes were considered for the O–H ground and excited states. The rotational profile for each O···O stretching vibration was simulated using the rigid asymmetric rotor model and each rotational line was fitted with a Lorentzian line shape function of FWHM of 0.1 cm^{-1}. The bandwidths of the fundamental vibrations for both the hydrogen bonded and free O–H starching vibrations were similar (35 cm^{-1}). However, with increasing energy, the bonded O–H stretching spread out more than did the free O–H stretching vibration. The third overtone of the O–H stretching vibration appeared remarkably broad (bandwidth ~300 cm^{-1}) compared to the free O–H stretching vibration (bandwidth ~40 cm^{-1}). More recently, Kjaergaard and co-workers (2011) revisited the fundamental and overtone vibrations of the hydrogen bonded O–H stretching, considering the coupling between the O–H stretch and acceptor wag with the aim of investigating the contribution of other large amplitude motions to the broadening of O–H stretching vibration.[72] With this new approach, they obtained comparatively narrower O–H stretch third overtone bands (bandwidth ~150 cm^{-1}) than what they reported previously (bandwidth ~300 cm^{-1}).

Dunn *et al*. (2006) reported anharmonic vibrational frequency calculations at the HF and MP2 levels of theory using different basis sets.[73] They showed that simple HF/6-31G* scaled frequencies for intramolecular and anharmonic intermolecular modes yielded good agreement with both the experimental data and accurate but more expensive MP2 calculations. A relatively higher value (20.5 cm^{-1}) for the standard deviation(sd) was obtained using harmonic frequency calculations at HF/6-31G* level with a scaling factor of 0.8929 compared to the more expensive MP2/aug-cc-pVTZ results, for which the sd was 15 cm^{-1}. Temelso *et al.* (2011) examined the vibrational anharmonicity of water clusters $(H_2O)_n$, n = 2-6, 8, 9 using the VPT2 method[74] and compared the calculated VPT2/aug-cc-pVDZ anharmonic frequencies with the MP2/aug-cc-pVDZ harmonic values scaled with different factors and with the experimentally measured values. In 2012, Kalescky *et al*. performed local and normal mode analysis of the hydrogen bonded stretching frequency at the CCSD(T)/CBS level of theory.[75] Local mode analysis yielded

a higher value (528 cm^{-1}) for the bond stretching frequency compared to the normal mode analysis (143 cm^{-1}). This large mismatch between the local and normal mode values was attributed to three effects: (*i*) the mass coupling due to the increased mass of bridging oxygen and hydrogen from the acceptor and donor parts, (*ii*) the large anharmonicity of the local compared to the normal mode and (*iii*) the strong coupling between the hydrogen bonded stretching and bending modes.

6. Classical interaction potentials

The significance of the water dimer PES in the development of classical, empirical potentials for water rests in the manner that the underlying intermolecular interactions are described in those models.[76] Following the extended discussion in the Introduction of that reference, classical potentials describing the total interaction in terms of the individual pair interactions (oftentimes termed additive or pairwise additive potentials) utilize an effective intermolecular PES, in which the many-body effects are folded in. Given the fact that these many-body, non-additive contributions (i.e. interactions due to triplets, quadruples and larger *n*-plets of monomers) for water are significant,[77–80] the effective dimer PES that pairwise additive potentials are based upon has very little resemblance to the true, gas phase dimer PES. On the other hand, classical potentials that attempt to explicitly account for the non-additive, many-body terms in water are based on the true, gas phase water dimer intermolecular PES and include the higher-order effects either explicitly (i.e. three-, four- and higher-body terms) or via an induction scheme, which accounts for the larger part of those effects to infinite order.

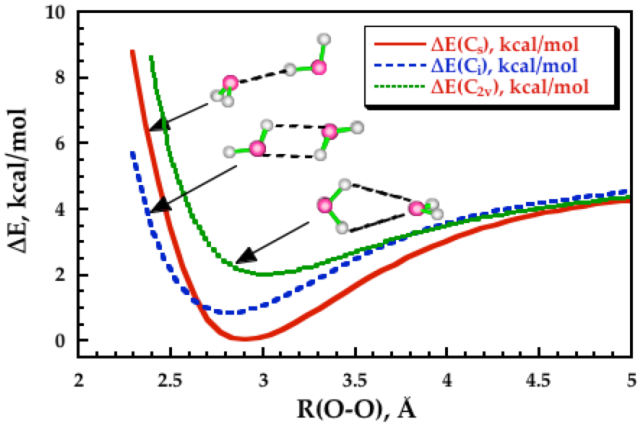

Figure 6. MEPs of the gas phase water dimer PES corresponding to the different approaches of the two molecules.

Minimum Energy Paths (MEPs) of the gas phase dimer PES corresponding to the different orientations of the two molecules have been determined from high level electronic structure calculations[76] and have been subsequently used in the parametrization of the "next generation" of interaction potentials for water that are suitable for nuclear statistical mechanical

simulations.[25, 60,81,82,24,83,84] These are shown in Figure 6 for the approach along a hydrogen bond (C_s symmetry, containing the global minimum) and two hydrogen bonds via the "cyclic" (C_i symmetry) or the "bifurcated" (C_{2v} symmetry) arrangements. It should be noted that at short O-O separations (i.e. less than 2.6 Å) the "bifurcated" arrangement is energetically more stable than other dimer arrangements under the previous symmetries.

Additionally, the lowest energy configurations of the MEPs under C_i and C_{2v} symmetries correspond to first order transition states and they are related to the interchange and bifurcation Vibrational-Rotational-Tunneling (VRT) splittings, experimentally measured by the Saykally group (Figure 7). As pointed out by Burnham and Xantheas[76], this topological feature (energetic

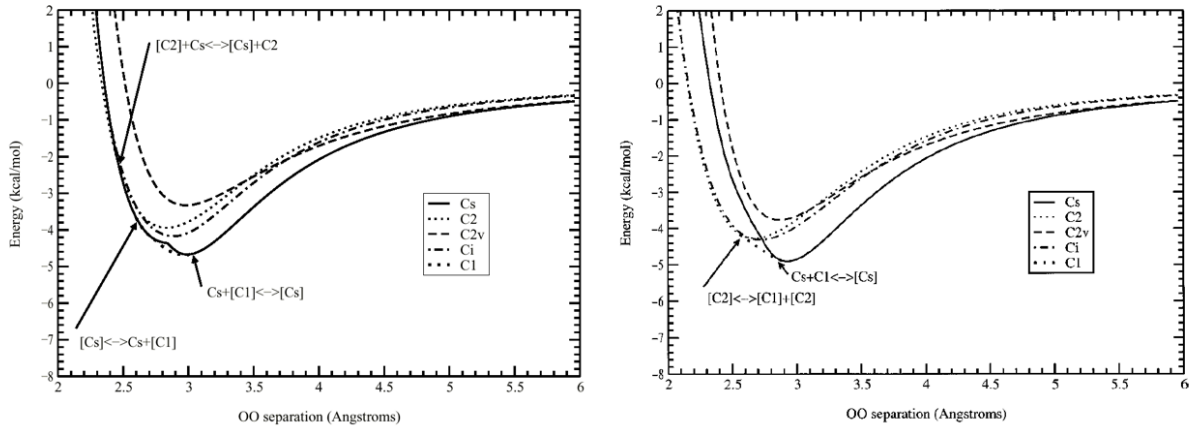

Figure 7. The fitting of the ASP-W potential to the experimentally measured VRT splittings results in the energetic stabilization of the "bifurcated" configurations for short O-O separations on the water dimer PES, a feature that was not well reproduced in the original potential.

stabilization of the "bifurcated" configurations at short O-O separations) is important in ensuring the accuracy of the 2-body interaction potential for water. Moreover, as Burnham and Xantheas have pointed out[76], the earlier fitting of the ASP-W interaction potential to the experimentally measured VRT splitting by Saykally, Leforestier and co-workers[85], which resulted in the ASP-VRT potential, mainly corrected this topological feature (energetic stabilization of the "bifurcated" arrangements for short O-O separations) on the water dimer PES (Figure 7, right panel), which was not well reproduced in the original version of the ASP-W potential (Figure 7, left panel).

The MEPs of Figure 6 have been used by Burnham and Xantheas in the development of the TTM2-F and TTM3-F interaction potentials for water,[25,60,82,84] and by Szalewicz and co-

workers during the development of the SAPT-5*s* and SDFT-5*s* interaction potentials for water,[86] whereas the above-mentioned topological feature has also been used by Paesani and co-workers in the development of the MB-pol potential.[83]

Several empirical potentials have been developed over the past three decades based on the water dimer PES and used to model larger clusters and the liquid. In general, these can be classified into those force fields that mainly aimed at reproducing the water dimer's salient spectroscopic features (such as infrared and VRT spectra) and those that relied on the dimer PES to account for the additive 2-body interaction in water and subsequently added the non-additive many-body effects. The work pursued before 2003 is documented by Keutsch and Saykally in a review article.[87] Given the limited scope of the present review, only progress made thereafter will be discussed here. Empirical potentials for water were developed by Jorgensen and named Transferable Intermolecular Potential Functions (TIPS).[88,89] Jorgensen and co-workers made several modifications over the years to the site-site type TIPS potentials after their initial development. This potential was reparametrized several times by addition of more than one active sites and geometrical parameters.[90] The geometric parameters were taken from gas phase experiment as in TIP3P and TIP4P for simulating liquid water. Classical Monte Carlo calculation was performed in the temperature range of -37.5 to 70°C and in the pressure range of 1 to 10,000 atm. The TIP5P model accurately simulates the density of liquid water with a density maximum at 4°C at a pressure of 1 atm and the error in temperature-dependent density was less than 1%. These effective pair potentials (TIP*n*P, n = 3, 4, 5) yield a nearly 0.3 Å shorter O-O distance and overestimate the dimerization energy by 1.0 kcal/mol for the water dimer compared to the *ab initio* results. These differences can be rationalized in terms of the fact that these TIP*n*P potentials are based on an effective, as opposed to the true, dimer PES, as mentioned earlier. For example, their monomer dipole moment is larger by almost 0.4 Debye than the gas phase monomer value to account for its increase in the condensed phase due to non-additive effects, leading to an enhanced dipole-dipole interaction that is part of the reason for the increase of the dimerization energy. Liu *et al*. (2006) studied rate constants for evaporation (K^{f}), condensation (K^{c}) and equilibrium (K^{EQ}) in case of water dimer and trimer using TIP4P and TIP5P models in combination with classical and quantum correction to these models.[91,92] The calculation is based on the estimation of potential mean force (PMF) which is related to the free energy associated with a reaction coordinate (here the intermolecular distance R). The PMF combined with

classical and dynamical nucleation theory (DNT) yielded the rate constants. Both classical and quantum corrected water models gave almost same kinetic constants for water dimer, but with increasing cluster size, the TIP4P model gives different kinetic values. This behavior was attributed to poor configuration sampling characteristic of the TIP4P model compared to TIP5P near the minima. The TIP5P result was nearly the same compared to that obtained with the TIP4P-FQ model, which considers charge fluctuation. In 2013, Tritzant-Martinez *et al*. constructed the free energy surface of a water dimer comprising rigid monomers using the Morse/Long Range (MLR) form for the long range and the metadynamics technique to obtain the PMF in the short range part of the surface.[93] The kinetic results obtained using metadynamics were in close correspondence with the values obtained with exact Monte Carlo or GS calculations. The MLR fitting reduces the computation cost of the data that the PMF needs to obtain over both short- and long-range.

Berendsen later introduced a Simple Point Charge (SPC) pair potential, which is slightly differently parametrized compared to Jorgensen's TIPS model (1981). This SPC potential was subsequently modified by Berendsen and several other groups (see Keutsch et al reviews[88, 94] for detailed description). Millot and Stone (1992) introduced an anisotropic site potential (ASP) for the water dimer constructed from rigid monomers[95] based on intermolecular perturbation theory. A number of modifications on this ASP potential were performed later on and the development and subsequent modifications are described in the Keutsch et al review articles.

Fellers *et al*. (1999) first used the Split Wigner Pseudo Spectral (SWPS) algorithm to obtain the VRT states of the water dimer on a six-dimensional (6-D) IPS.[96] The 6-D IPS was based on Millot and Stone's ASP-W pair potential and was called the VRT(ASP-W) potential.[97] This potential was further improved by several groups and used to obtain the dimerization constant $K_P(T)$, binding energy and the dimer partial pressure versus relative humidity over a large range of temperatures. Goldman and Saykally in 2004 reported a refined calculation of $K_P(T)$ using the more accurate VRT(ASP-W)III pair potential obtained by a third fitting of ASP-W potential to the far-IR and microwave data.[98] Several other thermodynamic parameters including ΔG, ΔH, ΔS, C_P, and C_V were estimated using the same potential. These authors reported a relatively lower value for the interaction energy (-20.078 kJ/mol) compared to the value reported by Curtiss *et al*.[5] Similarly the $K_P(T)$ value was also underestimated by the VRT(ASP-W)III potential. This was attributed to the non-rigid behavior of the water monomers.

Non-rigidity was reported to increase the $R_{O\text{-}O}$ distance and yielded a smaller value for the rotational constants, a fact that causes an increase in the $K_P(T)$ value. On the other hand, VRT(ASP-W)III considered rigid monomers which yielded a lower K_P value. Estimated values for other thermodynamic parameters yielded good agreement with the experimental results. The high concentration of water dimer in the atmosphere predicted using the VRT(ASP-W)III potential was confirmed by vibrational overtone measurements of $(H_2O)_2$ in the atmosphere by Pfeilsticker *et al*.[45]

Leforestier, Harrevelt and van der Avoird (2009) developed a 12-D flexible monomer potential to obtain the VRT energy levels of both $(H_2O)_2$ and $(D_2O)_2$ dimers.[99] This 12-d potential was fragmented in a (6-D) + (6-D) manner, wherein the fast intramolecular vibrations were separated adiabatically from the slow intermolecular ones. The result was compared with the 6-D potential with rigid monomers, wherein the monomers were kept fixed at either their equilibrium or the vibrationally averaged geometries. In the case of the 12-D potential with flexible monomers, the dissociation energy for $(H_2O)_2$ and $(D_2O)_2$ appears to be 24.0 cm^{-1} and 23.4 cm^{-1} higher compared to the 6-D rigid monomer model results, respectively. This difference was attributed to the lowering of the monomer zero-point energy in the flexible monomer model. On the other hand, the D_0 value appears to be 7.9 cm^{-1} and 2.9 cm^{-1} higher for $(H_2O)_2$ and $(D_2O)_2$, respectively, with the 6-D potential and the vibrationally averaged geometry, compared to the 12-D flexible monomer potential. Except for the acceptor tunneling splitting, a(K), all other constants, i.e. A, B+C appeared insensitive to the type of model used. These authors reported a 25% and 38% lowering of a(K) in the case of $(H_2O)_2$ and $(D_2O)_2$ dimers, respectively, with the flexible monomer model, in comparison to the rigid monomer model. But the a(K) value obtained with this flexible potential yielded a good agreement with experiment, with only 5% remaining errors for both dimer isotopologues.

Van der Avoird and co-workers (2010) obtained the VRT energy levels using a vibrationally averaged water dimer potential, in which they combined Shirin *et al*.'s (SHI08) monomer potential with Huang *et al*.'s HBB dimer potential.[100] The monomer potential SHI08 reproduces experimentally determined monomer bands up to 25,468 cm^{-1} for $J \leq 10$ with a very small standard deviation (0.1cm^{-1}). The result was compared with that from a 6-D water dimer potential, which used rigid monomers. The HBB+SHI08 yielded a 23 cm^{-1} higher value for the zero-point energy (ZPE) of the $(H_2O)_2$ dimer (9,899±5 cm^{-1}) compared to that with the HBB

dimer potential (9,8547±3cm^{-1}). This energy difference was attributed to the monomer ZPE difference. The dissociation energies D_e appeared 8.7 cm^{-1} lower for both $(H_2O)_2$ and $(D_2O)_2$, when computed with HBB+SHI08 compared to the HBB potential. The 6-D potential also shows the same trend for D_e for both the case of using equilibrium and vibrationally averaged monomer geometries. Additionally, the HBB+SHI08 potentials yielded a lower D_0 value compared to the result obtained with the HBB potential for both when using the equilibrium (3 cm^{-1} for $(H_2O)_2$ and 17 cm^{-1} $(D_2O)_2$) and vibrationally averaged monomer (VGS) geometry (4.8 cm^{-1} for $(H_2O)_2$ and 14.3 cm^{-1} for $(D_2O)_2$). This approach with monomers considered at either their vibrationally averaged geometry (VGS) or their vibrationally averaged potential (VAP) yielded an improved result for the tunneling splittings in the case of the ground state of both the H_2O and D_2O dimers, compared to the method where monomers are fixed at their equilibrium geometry (EQ).

Tennyson *et al*. (2012) estimated the contribution of the water dimer in the atmospheric continuum absorption in the near-infrared and visible wavelength range.[101] They relied on the HBB+SHI08 and the HBB2+SHI08 PESs, which they have previously used for VRT energy level calculations. Along with this potential, the monomer motion in a dimer is treated following different adiabatic separation approaches i.e. using (*i*) fixed monomer geometry, (*ii*) free-monomer, (*iii*) perturbed-monomer and (*iv*) coupled-monomer methods. The first approach considers fixed monomer coordinates to evaluate the dimer potential and is appropriate for a dimer wherein the monomers are in their vibrational ground state (VGS) and are not vibrationally excited. On the other hand, the free-monomer approach considers the full averaging over monomer internal coordinates. The perturbed-monomer approach considers the effect of dimer environment on the monomer wavefuntions. The monomer wavefunction is calculated at a fixed $R = R^{min}$ dimer grid point. Finally, in the coupled monomer approach, the perturbed monomer wave function is calculated at each R. The free-monomer approach either with a 6-D vibrational averaged potential (VAP) method or a (3+3)-D/GS method could not reproduce the dimer band origin. The free-monomer (3+3)-D and the coupled-monomer method yielded the best results. The HBB2+SHI08 potential was found to perform much better compared to the HBB+SHI08 potential. Except for the donor O–H stretching mode, the other stretching and bending fundamentals of the six intramolecular vibrational states obtained using the coupled-monomer approach yielded a good agreement with the HCAO and VPT2 results from Kjaergaard *et al*.[70] as well as matrix isolation and jet-cooled studies.[102,103] Leforestier recently (2012)

calculated infrared shifts of the water dimer using 12-D fully flexible HBB2 potential developed by Bowman and co-workers.[104] Bowman and co-workers developed this 12-D potential considering adiabatic separation between the 'fast' intra- and 'slow' inter-molecular modes, wherein the adiabatic intermolecular potential was obtained by solving the 6-D intramolecular subsystem for a fixed intermolecular geometry. The VRT energy levels and infrared shifts calculated with the HBB2 potential show good agreement with experiment, except for the bonded O–H and the asymmetric mode stretching fundamentals. This discrepancy with experiment was attributed to the nature of the potential. Both the O–H stretching and asymmetric fundamentals ([A] modes) are of high frequency (3,600 – 3,700 cm^{-1}) and involve distorted monomers, a fact that makes it more difficult to predict these frequencies accurately.

Leforestier, Szalewicz, and van der Avoird (2012) calculated water dimer spectra using the rigid monomer 12-D water dimer potential CCpol-8s in combination with the flexible SAPT-5s'fIR potential.[105] In this way, the monomer deformation effect[7] was included in the rigid CCpol-8s dimer potential. They obtained an accurate water dimer interaction energy, D_e=-21.0 kJ/mol, with this new flexible CCpol-8sf potential, compared to the benchmark value obtained by Tschumper *et al.*[106]. The error in other geometric parameters corresponding to the global minimum was also reduced to below 1% using this new flexible potential. The VRT energy levels and tunneling splittings obtained with the rigid CCpol potential yielded a good agreement with the experimental results, whereas the CCpol potential with the flexible monomer approximation did not significantly improve the agreement. A deviation of 4 cm^{-1} from the experimental value was obtained for the O–O stretch mode when calculated with the CCpol-8s flexible monomer, compared to the rigid monomer approximation, which yielded a difference of 0.3 cm^{-1}. This mismatch was attributed to the larger hydrogen bond length (0.06 Å) in the SAPT-5s′fIR model compared to the benchmark calculation by Tschumper *et al.*[21] Finally, the value of the $(H_2O)_2$ dissociation energy (1,108.2 cm^{-1}) obtained with the CCpol-8sf potential is only 3 cm^{-1} away above the experimental value (1,105±5 cm^{-1}) obtained by Reisler and co-workers[26] using their velocity map imaging experiment. On the other hand, the dimer dissociation energy obtained with the CCpol-8s rigid monomer potential is 11 cm^{-1} away from the experimental value[26] and indicates the importance of incorporating monomer flexibility in the calculation. In that respect, the CCpol-8sf potential exhibits similar accuracy with the previously developed HBB2 potential, which preceded the experimental determination of D_0.

Albertí *et al*. (2008) developed a model potential (AMPF) with parameters which are directly based on the physical properties, i.e. polarizability and dipole moment of small water clusters (dimer, trimer and tetramers).[107] In this model, the total interaction potential is derived as follows: $V = V_{vdW} + V_{ind} + V_{electr}$, where the V_{vdW} part is the summation of the repulsion (V_{rep}) and dispersion (V_{disp}) terms and is modeled using a modified Lennard-Jones (LJ) approach. The V_{ind} term is obtained from an asymptotic expression given by Buckingham[108] and the Columbic term V_{electr} is formulated from the dipole moment, which is constructed by considering a three-point charge distribution on each monomer within a given water cluster. The calculation was performed using the SPC geometry. The water dimer dissociation energy D_0=0.228 eV obtained with the AMPF potential is in good agreement with the value of 0.234 eV obtained from spectroscopic measurements.[109] On the other hand, the combined spectroscopic measurement and VRT(ASP-W) value is 0.213 eV. The $R_{O\text{-}O}$ distance obtained with the AMPF potential (2.81 Å) is slightly shorter than the value of 2.91 Å obtained from *ab initio* calculations.

Scribano and Leforestier (2007) used the 12-D (6-D + 6-D) water dimer potential to calculate the contribution of the water dimer absorption in the millimeter and far infrared region within the temperature range of 276-310K.[110] The transition dipole moment was calculated up to 750 cm^{-1} and the population up to the $J = K = 5$ energy levels was considered. A frequency-dependent water dimer absorption contribution was reported, wherein the maximum absorption was found within the 0-10 cm^{-1} range and only a 3% contribution was found at the highest frequency, 944 cm^{-1}.

Moraweitz *et al*. employed full-dimensional neural network (NN) calculation to obtain the binding energy, vibrational frequency and geometric parameters of the water dimer and the result was compared with DFT calculations.[111] In the NN method, the energy of each atom depends on a local environment, which is defined by a sphere of cut-off radius R_c and considers the effect of neighboring atoms inside that sphere. The convergence of the NN result depends on the choice of the R_c value. In the full dimensional PES, the total energy of a system is represented as $E_{tot} = E_{short} + E_{elec.}$, where E_{elec} represents the long range electrostatic contribution. . The relative binding energies for the global minimum and nine stationary points obtained with the R_c = 10 Å value yielded excellent match with the reference DFT calculation. The value of the absolute interaction energy at the global minimum obtained with the NN method was reported at

-225.6 meV, which is barely different from the DFT value of -225.0 meV. The vibrational frequencies and geometric parameters of the dimer were also well reproduced by this NN PES.

On the other end of the water potential development effort that involves many-body force fields, the water dimer PES is the starting point in the process. In 2002, Xantheas and co-workers advocated the use of *ab initio* electronic structure results to parametrize the two-body water interaction (proposed earlier by Clementi and co-workers during the development of MCY and MCY-CI potentials[112,113]) but in conjunction with nuclear statistical mechanical (instead of classical) molecular dynamics simulations for condensed phase simulations. The goal was to develop a full dimensional water potential which can accurately describe interactions from the water dimer up to liquid water. These authors relied on the MEPs of Figure 6 and used about 45 points obtained at the MP2 level of theory to parametrize an earlier Thole-type Model (TTM).[114] The resulting TTM2-R (rigid)[82] and TTM2-F (flexible)[60,84] models have been used in conjunction with Centroid Molecular Dynamics simulations to obtain the macroscopic properties of liquid water.[115–117] The intramolecular part of the PES was based on the highly accurate Partridge-Schwenke water monomer PES[118] which has a non-linear dipole moment surface[119] and it was implemented using a scheme to allow for intramolecular charge transfer between the hydrogen and oxygen atoms.[120] This potential was furthe extended to incorporate just one polarizable site per monomer to describe the vibrational spectra of water clusters and liquid water.[25] These ideas and approach gave rise to the subsequent development of the WHBB-2 and MB-pol potentials by the Bowman and Paesani groups, respectively.

Paesani and co-workers subsequently developed a full-dimensional HBB2-pol model and used it in the simulation of structural and dynamical properties of water.[121] The HBB2-pol model is also based on the many-body expansion of molecular interactions, in which the 1-body term was taken from the spectroscopically accurate PES developed by Partridge and Schwenke[118] as in the earlier case for the TTM models. The 2-body interaction at short range is represented by HBB2-pol, which at long range i.e. between 5.5 Å and 7.5 Å, asymptotically changes to electrostatic and dispersion interaction. At short range the electrostatic repulsion was accounted by an explicit 3-body term. The induction part was taken into account through Thole-type point polarizable dipoles, as in the case of the earlier TTM models. The 2-body and 3-body interaction energies obtained with this HBB2-pol model yielded a good agreement with those obtained at the CCSD(T)/aug-cc-pVTZ level. Several cluster and liquid water macroscopic properties were

reported using this model. For instance, PIMD simulations with this potential reported that in liquid water each water molecule is connected to three other water molecules and 57% are double donors and 38% are single donors.

Babin, Leforestier and Paesani subsequently developed the flexible monomer MB-pol potential which was also based on the many-body expansion of the total interaction.[122] They mainly focused on the accurate description of the two-body term, $V^{(2B)}$, i.e. the interaction between two water molecules. The two-body term was cast as $V^{(2B)}(x_a, x_b) = V^{(2B)}_{short}(x_a, x_b) + V^{(2B)}_{long}(x_a, x_b)$, where the first term describes the short-range and the second one the long-range interaction. The long-range term mainly constitutes of electrostatic (both permanent and induced moments), dispersion and induction components. The permanent moment was modeled following the TTM model where point charges were derived from the Partridge and Schwenke *ab initio* monomer dipole moment surface[118]. The induction component was modeled by a modified version of the TTM-type framework and the dispersion contribution was modeled using damped r^{-6} and r^{-8} terms. The short-range term comprises permutationally invariant polynomials. The two-body term $V^{(2B)}$ was constructed by fitting 40,000 water dimer energies calculated at the CCSD(T)/CBS level. The energies at stationary point and nine saddle points obtained using MB-pol method yielded a good agreement with the CCSD(T)/CBS results. The VRT dimer spectra, the energy levels and tunneling splittings obtained with this flexible MB-pol method yielded a very good agreement with the experimental measurements obtained by the Saykally group.

In a following article, Medders, Babin and Paesani reported classical and quantum simulations of liquid water with the MB-pol potential.[123] Like the two-body term, the 3-body term was cast as $V^{(3B)}(x_a, x_b, x_c) = V^{(3B)}_{short}(x_a, x_b, x_c) + V^{(3B)}_{ind}(x_a, x_b, x_c)$, where the short-range expansion was represented by permutationally invariant polynomials. Like for the 2-body term, the 3-body term was also derived by fitting *ab initio* energies obtained from CCSD(T)/CBS and CCSD(T)/ aug-cc-pVTZ calculations. Both path-integral molecular dynamics (PIMD) and centroid molecular dynamics (CMD) simulations were performed to obtain structural, dynamical and thermodynamic properties of liquid water at T=298.15K and P=1atm. Among the different thermodynamic properties, the heat of vaporization of liquid water obtained using quantum PIMD/classical simulations appeared lower/higher than the experimental value.

Szalewicz and co-workers recently (2014) described a potential for water based on a rigid monomer approximation.[124] The PES was developed by fitting 71,456 trimer interaction energies obtained with CCSD(T)/ aug-cc-pVTZ ab initio theoretical calculation. This three-body potential along with the modified two body effect and higher body (4 and higher) polarization effect were used together with the CCpol23+ potential to predict the energetics of the trimer, hexamer and 24-mer water clusters.

Acknowledgements: AM & RJS are part of the Berkeley terahertz project, which was previously supported by the Chemical Structure, Dynamics, and Mechanisms-A Division of the National Science Foundation under Grant No. 1300723. This project is currently supported by the CALSOLV collaboration, an affiliate program of RESOLV (Ruhr-Unversität Bochum). SSX acknowledges support from the U.S. Department of Energy, Office of Science, Office of Basic Energy Sciences, Division of Chemical Sciences, Geosciences and Biosciences at Pacific Northwest National Laboratory. Battelle operates the Pacific Northwest National Laboratory for the U.S. Department of Energy.

References

(1) Morokuma, K.; Pedersen, L. Molecular Orbital Studies of Hydrogen Bonds. An Ab Initio Calculation for Dimeric H2O. *J. Chem. Phys.* **1968**, *48* (7), 3275–3282.
(2) Scheiner, S. Ab Initio Studies of Hydrogen Bonds: The Water Dimer Paradigm. *Annu. Rev. Phys. Chem.* **1994**, *45*, 23–56.
(3) Dyke, T. R.; Mack, K. M.; Muenter, J. S. The Structure of Water Dimer from Molecular Beam Electric Resonance Spectroscopy. *J. Chem. Phys.* **1977**, *66* (2), 498.
(4) Odutola, J. A.; Dyke, T. R. Partially Deuterated Water Dimers : Microwave Spectra and Structure. *J. Chem. Phys.* **1980**, *72* (9), 5062–5070.
(5) Curtiss, L. A.; Frurip, D. J.; Blander, M. Studies of Molecular Association in H_2O and D_2O Vapors by Measurement of Thermal Conductivity. *J. Chem. Phys.* **1979**, *71* (6), 2703–2711.
(6) van Duijneveldt-van de Rijdt, J. G. C. M.; van Duijneveldt, F. B. Convergence to the Basis-Set Limit in Ab Initio Calculations at the Correlated Level on the Water Dimer. *J. Chem. Phys.* **1992**, *97* (7), 5019.
(7) Xantheas, S. S. On the Importance of the Fragment Relaxation Energy Terms in the Estimation of the Basis Set Superposition Error Correction to the Intermolecular Interaction Energy. *J. Chem. Phys.* **1996**, *104* (21), 8821.
(8) Schütz, M.; Brdarski, S.; Widmark, P.; Lindh, R.; Karlström, G. The Water Dimer

Interaction Energy: Convergence to the Basis Set Limit at the Correlated Level. *J. Chem. Phys.* **1997**, *107* (12), 4597–4605.
(9) Schütz, M.; Rauhut, G.; Werner, H.-J. Local Treatment of Electron Correlation in Molecular Clusters: Structures and Stabilities of $(H_2O)_N$, N = 2−4. *J. Phys. Chem. A* **1998**, *102* (29), 5997–6003.
(10) Famulari, a.; Raimondi, M.; Sironi, M.; Gianinetti, E. Ab Initio MO–VB Study of Water Dimer. *Chem. Phys.* **1998**, *232* (3), 289–298.
(11) Bandyopadhyay, P.; Ten-No, S.; Iwata, S. Ab Initio Monte Carlo Simulation Using Multicanonical Algorithm: Temperature Dependence of the Average Structure of Water Dimer. *Mol. Phys.* **1999**, *96* (3), 349–358.
(12) Hobza, P.; Bludsky, O. Reliable Theoretical Treatment of Molecular Clusters : Counterpoise-Corrected Potential Energy Surface and Anharmonic Vibrational Frequencies of the Water Dimer. *Phys. Chem. Chem. Phys.* **1999**, *1*, 3073–3078.
(13) Halkier, A.; Koch, H.; Jorgensen, P.; Christiansen., O.; Nielsen, I. M. B.; Helgaker, T. A Systematic Ab Initio Study of the Water Dimer in Hierarchies\rof Basis Sets and Correlation Models. *Theor. Chem. Acc.* **1997**, *97*, 150–157.
(14) Halkier, A.; Klopper, W.; Helgaker, T.; Jørgensen, P.; Taylor, P. R. Basis Set Convergence of the Interaction Energy of Hydrogen-Bonded Complexes. *J. Chem. Phys.* **1999**, *111* (20), 9157.
(15) Klopper, W.; M. van Duijneveldt-van de Rijdt, J. G. C.; van Duijneveldt, F. B. Computational Determination of Equilibrium Geometry and Dissociation Energy of the Water Dimer. *Phys. Chem. Chem. Phys.* **2000**, *2* (10), 2227–2234.
(16) Grigorenko, B. L.; Nemukhin, A. V.; Topol, I. A.; Burt, S. K. Hydrogen Bonding at the Diatomics-in-Molecules Level : Water Clusters. *J. Chem. Phys.* **2000**, *113* (7), 2638.
(17) Mas, E. M.; Bukowski, R.; Szalewicz, K.; Groenenboom, G. C.; Wormer, P. E. S.; van der Avoird, A. Water Pair Potential of near Spectroscopic Accuracy. I. Analysis of Potential Surface and Virial Coefficients. *J. Chem. Phys.* **2000**, *113* (16), 6687.
(18) Feyereisen, M. W.; Feller, D.; Dixon, D. a. Hydrogen Bond Energy of the Water Dimer. *J. Phys. Chem.* **1996**, *100* (8), 2993–2997.
(19) Torheyden, M.; Jansen, G. A New Potential Energy Surface for the Water Dimer Obtained from Separate Fits of Ab Initio Electrostatic , Induction , Dispersion and Exchange Energy Contribution. *Mol. Phys.* **2006**, *104* (13-14), 2101–2138.
(20) Smith, B. J.; Swanton, D. J.; Pople, J. A.; Schaefer, H. F.; Radom, L. Transition Structures for the Interchange of Hydrogen Atoms within the Water Dimer. *J. Chem. Phys.* **1990**, *92* (2), 1240.
(21) Tschumper, G. S.; Leininger, M. L.; Hoffman, B. C.; Valeev, E. F.; Schaefer, H. F.; Quack, M. Anchoring the Water Dimer Potential Energy Surface with Explicitly Correlated Computations and Focal Point Analyses. *J. Chem. Phys.* **2002**, *116* (2), 690–701.
(22) Huang, X.; Braams, B. J.; Bowman, J. M. Ab Initio Potential Energy and Dipole Moment Surfaces of (H2O)2 †. *J. Phys. Chem. A* **2006**, *110*, 445–451.
(23) Wang, Y.; Carter, S.; Braams, B. J.; Bowman, J. M. MULTIMODE Quantum Calculations of Intramolecular Vibrational Energies of the Water Dimer and Trimer Using *Ab Initio* - Based Potential Energy Surfaces. *J. Chem. Phys.* **2008**, *128* (7), 071101.
(24) Shank, A.; Wang, Y.; Kaledin, A.; Braams, B. J.; Bowman, J. M. Accurate Ab Initio and "hybrid" Potential Energy Surfaces, Intramolecular Vibrational Energies, and Classical Ir

Spectrum of the Water Dimer. *J. Chem. Phys.* **2009**, *130* (14), 144314.
(25) Fanourgakis, G. S.; Xantheas, S. S. Development of Transferable Interaction Potentials for Water. V. Extension of the Flexible, Polarizable, Thole-Type Model Potential (TTM3-F , v. 3.0) to Describe the Vibrational Spectra of Water Clusters and Liquid Water. *J. Chem. Phys.* **2008**, *128* (7), 074506.
(26) Rocher-Casterline, B. E.; Ch'ng, L. C.; Mollner, A. K.; Reisler, H. Communication: Determination of the Bond Dissociation Energy (D0) of the Water Dimer, $(H_2O)_2$, by Velocity Map Imaging. *J. Chem. Phys.* **2011**, *134* (21), 211101.
(27) Wang, Y.; Bowman, J. M. Towards an Ab Initio Flexible Potential for Water, and Post-Harmonic Quantum Vibrational Analysis of Water Clusters. *Chem. Phys. Lett.* **2010**, *491* (1-3), 1–10.
(28) Bukowski, R.; Szalewicz, K.; Groenenboom, G. C.; van der Avoird, A. Polarizable Interaction Potential for Water from Coupled Cluster Calculations. I. Analysis of Dimer Potential Energy Surface. *J. Chem. Phys.* **2008**, *128* (9), 094313.
(29) Bukowski, R.; Szalewicz, K.; Groenenboom, G. C.; van der Avoird, A. Polarizable Interaction Potential for Water from Coupled Cluster Calculations. II. Applications to Dimer Spectra, Virial Coefficients, and Simulations of Liquid Water. *J. Chem. Phys.* **2008**, *128* (9), 094314.
(30) Amadei, A.; Aschi, M.; Spezia, R.; Nola, A. D. A First Principle Polarizable Water Model for Molecular Simulations: Application to a Water Dimer. *J. Mol. Liq.* **2002**, *101*, 181–198.
(31) D'Alessandro, M.; Di Lella, a.; Aschi, M.; Di Nola, a.; Amadei, a. Theoretical Characterization of Structural and Energetical Properties of Water Clusters, by Means of a Simple Polarizable Water Hamiltonian. *J. Mol. Liq.* **2008**, *142* (1-3), 111–117.
(32) Lane, J. R. CCSDTQ Optimized Geometry of Water Dimer. *J. Chem. Theory Comput.* **2013**, *9* (1), 316–323.
(33) Howard, J. C.; Tschumper, G. S. Benchmark Structures and Harmonic Vibrational Frequencies Near the CCSD(T) Complete Basis Set Limit for Small Water Clusters: (H2O)n = 2, 3, 4, 5, 6. *J. Chem. Theory Comput.* **2015**, *11* (5), 2126–2136.
(34) Slanina, Z.; Filip, U.; Jean-francois, C. A Computational Evaluation of the Water-Dimer Populations in Saturated Steam Recommended for Applications to the Earth ' S , Planetary and Cometary Atmospheres *. *J. Mol. Struct.* **1992**, *270*, 1–9.
(35) Slanina, Z. Pressure Enhancement of Gas-Phase Water Oligomer Populations : A RRHO MCY-B / EPEN Computational Study. *Z. Phys. D* **1987**, *186* (5), 181–186.
(36) Slanina, Z. Temperature Enhancement Of Water-Oligomer Populations In Saturated Aqueous Vapour. *Thermochim. Acta* **1987**, *116*, 161–169.
(37) Slanina, Z. Computational Studies of Water Clusters: Temperature, Pressure, and Saturation Effects on Cluster Fractions within the RRHO MCY-B/EPEN Steam*. *J. Mol. Struct.* **1990**, *273*, 81–92.
(38) Slanina, Z. A Comparative Study of the Water-Dimer Gas-Phase Thermodynamics in the BJH- and MCYGtype Flexible Potentials *. *Chem. Phys.* **1991**, *150*, 321–329.
(39) Slanina, Z.; Crifo, J. F. A Refined Evaluation of the Gas-Phase Water-Dimerization Equilibrium Constant within Non-Rigid BJH- and MCY-Type Potentials. *Int. J. Thermophys.* **1992**, *13* (3), 465–476.
(40) Slanina, Z.; Uhlík, F.; Saito, A. T.; Osawa, E. Computing Molecular Complexes in Earth's and Other Atmospheres. *Phys. Chem. Earth, Part C Solar, Terr. Planet. Sci.* **2001**, *26* (7),

505–511.
(41) Slanina, Z. Clustering , Saturated Vapors , and the Atmosphere. *J. Chinese Chem. Soc.* **2003**, *50*, 607–610.
(42) Slanina, Z.; Uhlík, F.; Lee, S. L.; Nagase, S. Computational Modelling for the Clustering Degree in the Saturated Steam and the Water-Containing Complexes in the Atmosphere. *J. Quant. Spectrosc. Radiat. Transf.* **2006**, *97* (3), 415–423.
(43) Uhlik, F.; Slanina, Z.; Lee, S. L.; Wang, B. C.; Adamowicz, L.; Nagase, S. Water-Dimer Stability and Its Fullerene Encapsulations. *J. Comput. Theor. Nanosci.* **2015**, *12* (6), 959–964.
(44) Slanina, Z.; Uhlík, F.; Lu, X.; Akasaka, T.; Lemke, K. H.; Seward, T. M.; Nagase, S.; Adamowicz, L. Calculations of the Water-Dimer Encapsulations into C 84. *Fullerenes, Nanotub. Carbon Nanostructures* **2016**, *24* (1), 1–7.
(45) Pfeilsticker, K.; Lotter, A.; Peters, C.; Bosch, H. Atmospheric Detection of Water Dimers via near-Infrared Absorption. *Science (80-.).* **2003**, *300* (5628), 2078.
(46) Ptashnik, I. V.; Smith, K. M.; Shine, K. P.; Newnham, D. a. Laboratory Measurements of Water Vapour Continuum Absorption in Spectral Region 5000–5600 cm^{-1}: Evidence for Water Dimers. *Q. J. R. Meteorol. Soc.* **2004**, *130* (602), 2391–2408.
(47) Lemke, K. H.; Seward, T. M. Ab Initio Investigation of the Structure, Stability, and Atmospheric Distribution of Molecular Clusters Containing H_2O, CO_2 , and N_2O. *J. Geophys. Res.* **2008**, *113* (D19), D19304.
(48) Ruscic, B. Active Thermochemical Tables: Water and Water Dimer. *J. Phys. Chem. A* **2013**, *117* (46), 11940–11953.
(49) Dunn, M. E.; Pokon, E. K.; Shields, G. C. Thermodynamics of Forming Water Clusters at Various Temperatures and Pressures by Gaussian-2, Gaussian-3, Complete Basis Set-QB3, and Complete Basis Set-APNO Model Chemistries; Implications for Atmospheric Chemistry. *J. Am. Chem. Soc.* **2004**, *126* (8), 2647–2653.
(50) Wu, X.; Vargas, M. C.; Nayak, S. Towards Extending the Applicability of Density Functional Theory to Weakly Bound Systems. *J. Chem. Phys.* **2001**, *115* (19), 8748–8757.
(51) Misquitta, A. J.; Jeziorski, B.; Szalewicz, K. Dispersion Energy from Density-Functional Theory Description of Monomers. *Phys. Rev. Lett.* **2003**, *91* (3), 033201.
(52) Xu, X.; Goddard, W. A. From The Cover: The X3LYP Extended Density Functional for Accurate Descriptions of Nonbond Interactions, Spin States, and Thermochemical Properties. *Proc. Natl. Acad. Sci.* **2004**, *101* (9), 2673–2677.
(53) Xu, X.; Goddard, W. A. I. Bonding Properties of the Water Dimer: A Comparative Study of Density Functional Theories. *J. Phys. Chem. A* **2004**, *108* (12), 2305–2313.
(54) Csonka, G. I.; Ruzsinszky, A.; Perdew, J. P. Proper Gaussian Basis Sets for Density Functional Studies of Water Dimers and Trimers Ga. *J. Phys. Chem. B* **2005**, *109*, 21471–21475.
(55) Glendening, E. D. Natural Energy Decomposition Analysis: Extension to Density Functional Methods and Analysis of Cooperative Effects in Water Clusters. *J. Phys. Chem. A* **2005**, *109* (51), 11936–11940.
(56) Cabral do Couto, P.; Estácio, S. G.; Costa Cabral, B. J. The Kohn-Sham Density of States and Band Gap of Water: From Small Clusters to Liquid Water. *J. Chem. Phys.* **2005**, *123* (5), 054510.
(57) Anderson, J. A.; Tschumper, G. S. Characterizing the Potential Energy Surface of the Water Dimer with DFT : Failures of Some Popular Functionals for Hydrogen Bonding. *J.*

Phys. Chem. A **2006**, *110*, 7268–7271.
(58) Thar, J.; Hovorka, R.; Kirchner, B. Basis Set Superposition Error along the Free-Energy Surface of the Water Dimer. *J. Chem. Theory Comput.* **2007**, *3* (4), 1510–1517.
(59) Shields, G. C.; Kirschner, K. N. The Limitations of Certain Density Functionals in Modeling Neutral Water Clusters. *Synth. React. Inorganic, Met. Nano-Metal Chem.* **2008**, *38* (1), 32–39.
(60) Burnham, C. J.; Xantheas, S. S. Development of Transferable Interaction Models for Water. IV. A Flexible, All-Atom Polarizable Potential (TTM2-F) Based on Geometry Dependent Charges Derived from an Ab Initio Monomer Dipole Moment Surface. *J. Chem. Phys.* **2002**, *116* (12), 5115.
(61) Mattsson, A. E.; Mattsson, T. R. AM05 Density Functional Applied to the Water Molecule , Dimer , and Bulk Liquid †. *J. Chem. Theory Comput.* **2009**, *5*, 887–894.
(62) Santra, B.; Michaelides, A.; Scheffler, M. Coupled Cluster Benchmarks of Water Monomers and Dimers Extracted from Density-Functional Theory Liquid Water : The Importance of Monomer. *J. Chem. Phys.* **2009**, *131*, 124509.
(63) Khaliullin, R. Z.; Bell, A. T.; Head-gordon, M. Electron Donation in the Water – Water Hydrogen Bond. *Chem. A Eur. J.* **2009**, *15*, 851–855.
(64) Plumley, J. A.; Dannenberg, J. J. A Comparison of the Behavior of Functional/basis Set Combinations for Hydrogen-Bonding in the Water Dimer with Emphasis on Basis Set Superposition Error. *J. Comput. Chem.* **2011**, *32* (8), 1519–1527.
(65) Hus, M.; Urbic, T. Strength of Hydrogen Bonds of Water Depends on Local Environment. *J. Chem. Phys.* **2012**, *136*, 144305.
(66) Jung, J. O.; Gerber, R. B. Vibrational Wave Functions and Spectroscopy of $(H_2O)_n$, n=2,3,4,5: Vibrational Self-Consistent Field with Correlation Corrections. *J. Chem. Phys.* **1996**, *105* (23), 10332–10348.
(67) Low, G. R.; Kjaergaard, H. G. Calculation of OH-Stretching Band Intensities of the Water Dimer and Trimer. *J. Chem. Phys.* **1999**, *110* (18), 9104–9115.
(68) Schofield, D. P.; Kjaergaard, H. G. Calculated OH-Stretching and HOH-Bending Vibrational Transitions in the Water Dimer. *Phys. Chem. Chem. Phys.* **2003**, *5* (15), 3100.
(69) Schofield, D. P.; Lane, J. R.; Kjaergaard, H. G. Hydrogen Bonded OH-Stretching Vibration in the Water Dimer. *J. Phys. Chem. A* **2007**, *111*, 567–572.
(70) Kjaergaard, H. G.; Garden, A. L.; Aarhus, C.; Chaban, G. M.; Gerber, R. B.; Matthews, D. A.; Stanton, J. F. Calculation of Vibrational Transition Frequencies and Intensities in Water Dimer : Comparison of Different Vibrational Approaches. *J. Phys. Chem. A* **2008**, *112*, 4324–4335.
(71) Garden, A. L.; Halonen, L.; Kjaergaard, H. G. Calculated Band Profiles of the OH-Stretching Transitions in Water Dimer. *J. Phys. Chem. A* **2008**, *112*, 7439–7447.
(72) Garden, A. L.; Halonen, L.; Kjaergaard, H. G. Widening of the Hydrogen Bonded OH-Streching Bands due to the Wagging and OO-Stretching Modes in H2O·H2O. *Chem. Phys. Lett.* **2011**, *513* (4-6), 167–172.
(73) Dunn, M. E.; Evans, T. M.; Kirschner, K. N.; Shields, G. C. Prediction of Accurate Anharmonic Experimental Vibrational Frequencies for Water Clusters , $(H_2O)_N$, N =2 - 5. *J. Phys. Chem. A* **2006**, *110*, 303–309.
(74) Temelso, B.; Shields, G. C. The Role of Anharmonicity in Hydrogen-Bonded Systems : The Case of Water Clusters. *J. Chem. Theory Comput.* **2011**, *7*, 2804–2817.
(75) Kalescky, R.; Zou, W.; Kraka, E.; Cremer, D. Local Vibrational Modes of the Water

Dimer – Comparison of Theory and Experiment. *Chem. Phys. Lett.* **2012**, *554*, 243–247.
(76) Burnham, C. J.; Xantheas, S. S. Development of Transferable Interaction Models for Water. I. Prominent Features of the Water Dimer Potential Energy Surface. *J. Chem. Phys.* **2002**, *116* (4), 1479–1492.
(77) Xantheas, S. S. Significance of Higher-Order Many-Body Interaction Energy Terms in Water Clusters and Bulk Water. *Philos. Mag. B Phys. Condens. Matter; Stat. Mech. Electron. Opt. Magn. Prop.* **1996**, *73* (1), 107–115.
(78) Xantheas, S. S. *Ab Initio* Studies of Cyclic Water Clusters $(H_2O)_N$, N =1–6. II. Analysis of Many-body Interactions. *J. Chem. Phys.* **1994**, *100* (10), 7523–7534.
(79) Xantheas, S. S.; Dunning, T. H. The Structure of the Water Trimer from *Ab Initio* Calculations. *J. Chem. Phys.* **1993**, *98* (10), 8037–8040.
(80) Xantheas, S. S. Cooperativity and Hydrogen Bonding Network in Water Clusters. *Chem. Phys.* **2000**, *258* (2-3), 225–231.
(81) Xantheas, S. S.; Burnham, C. J.; Harrison, R. J. Development of Transferable Interaction Models for Water. II. Accurate Energetics of the First Few Water Clusters from First Principles. *J. Chem. Phys.* **2002**, *116* (4), 1493–1499.
(82) Burnham, C. J.; Xantheas, S. S. Development of Transferable Interaction Models for Water. III. Reparametrization of an All-Atom Polarizable Rigid Model (TTM2–R) from First Principles. *J. Chem. Phys.* **2002**, *116* (4), 1500–1510.
(83) Babin, V.; Leforestier, C.; Paesani, F. Development of a "First Principles" Water Potential with Flexible Monomers: Dimer Potential Energy Surface, VRT Spectrum, and Second Virial Coefficient. *J. Chem. Theory Comput.* **2013**, *9* (12), 5395–5403.
(84) Fanourgakis, G. S.; Xantheas, S. S. The Flexible, Polarizable, Thole-Type Interaction Potential for Water (TTM2-F) Revisited. *J. Phys. Chem. A* **2006**, *110* (11), 4100–4106.
(85) Fellers, R. S. Spectroscopic Determination of the Water Pair Potential. *Science (80-.).* **1999**, *284* (5416), 945–948.
(86) Bukowski, R.; Szalewicz, K.; Groenenboom, G.; van der Avoird, A. Interaction Potential for Water Dimer from Symmetry-Adapted Perturbation Theory Based on Density Functional Description of Monomers. *J. Chem. Phys.* **2006**, *125* (4), 044301.
(87) Keutsch, F. N.; Cruzan, J. D.; Saykally, R. J. The Water Trimer. *Chem. Rev.* **2003**, *103* (7), 2533–2577.
(88) Jorgensen, W. I. Transferable Intermolecular Potential Functions for Water, Alcohols, and Ethers. Application to Liquid Water'. *J. Am. Chem. Soc.* **1981**, *103*, 335–340.
(89) Jorgensen, W. L. Revised TIPS for Simulations of Liquid Water and Aqueous Solutions. *J. Chem. Phys.* **1982**, *77* (8), 4156.
(90) Mahoney, M. W.; Jorgensen, W. L. A Five-Site Model for Liquid Water and the Reproduction of the Density Anomaly by Rigid, Nonpolarizable Potential Functions. *J. Chem. Phys.* **2000**, *112* (20), 8910.
(91) Liu, J.; Yang, L.; Doren, D. J. Free Energy Perturbation and Dynamical Nucleation Study of Water Dimer and Trimer through TIP5P Water Model. *Chem. Phys. Lett.* **2006**, *417* (1-3), 63–71.
(92) Liu, J.; Yang, L.; Doren, D. J. Comparison of TIP5P Water Model and TIP4P Water Model in Cluster Nucleation Kinetics Study through Umbrella Sampling and Free Energy Perturbation. *Chem. Phys.* **2006**, *323* (2-3), 579–586.
(93) Tritzant-Martinez, Y.; Zeng, T.; Broom, A.; Meiering, E.; Le Roy, R. J.; Roy, P. On the Analytical Representation of Free Energy Profiles with a Morse/long-Range Model:

Application to the Water Dimer. *J. Chem. Phys.* **2013**, *138* (23), 234103.
(94) Keutsch, F. N.; Cruzan, J. D.; Saykally, R. J. The Water Trimer. *Chem. Rev.* **2003**, *103* (7), 2533–2578.
(95) Millot, C.; Stone, A. J. Towards an Accurate Intermolecular Potential for Water. *Mol. PhysicsAn Int. J. Interface Between Chem. Phys.* **1992**, *77* (3), 439–462.
(96) Fellers, R. S.; Braly, L. B.; Saykally, R. J.; Leforestier, C. Fully Coupled Six-Dimensional Calculations of the Water Dimer Vibration-Rotation- Tunneling States with Split Wigner Pseudospectral Approach . II . Improvements and Tests of Additional Potentials Fully Coupled Six-Dimensional Calculations of the Water Dim. *J. Chem. Phys.* **1999**, *110*, 6306.
(97) Millot, C.; Soetens, J.; Costa, T. C. M.; Hodges, M. P.; Stone, A. J. Revised Anisotropic Site Potentials for the Water Dimer and Calculated Properties. *J. Phys. Chem. A* **1998**, *102* (97), 754–770.
(98) Goldman, N.; Leforestier, C.; Saykally, R. J. Water Dimers in the Atmosphere II: Results from the VRT(ASP-W)III Potential Surface. *J. Phys. Chem. A* **2004**, *108*, 787–794.
(99) Leforestier, C.; Harrevelt, R. V.; Avoird, A. Van Der. Vibration - Rotation - Tunneling Levels of the Water Dimer from an Ab Initio Potential Surface with Flexible Monomers. *J. Phys. Chem. A* **2009**, *113*, 12285–12294.
(100) Kelly, R. E. a.; Tennyson, J.; Groenenboom, G. C.; van der Avoird, A. Water Dimer Vibration–rotation Tunnelling Levels from Vibrationally Averaged Monomer Wavefunctions. *J. Quant. Spectrosc. Radiat. Transf.* **2010**, *111* (9), 1262–1276.
(101) Tennyson, J.; Barber, M. J.; Kelly, R. E. a. An Adiabatic Model for Calculating Overtone Spectra of Dimers such as $(H_2O)_2$. *Philos. Trans. A. Math. Phys. Eng. Sci.* **2012**, *370* (1968), 2656–2674.
(102) Bouteiller, Y.; Perchard, J. P. The Vibrational Spectrum of $(H_2O)_2$: Comparison between Anharmonic Ab Initio Calculations and Neon Matrix Infrared Data between 9000 and 90 cm^{-1}. *Chem. Phys.* **2004**, *305* (1-3), 1–12.
(103) Huang, Z. S.; Miller, R. E. High-Resolution near-Infrared Spectroscopy of Water Dimer Z. *J. Chem. Phys.* **1989**, *91* (11), 6613–6631.
(104) Leforestier, C. Infrared Shifts of the Water Dimer from the Fully Flexible Ab Initio HBB2 Potential. *Philos. Trans. R. Soc. A, Math. Phys. Eng. Sci.* **2012**, *370* (1968), 2675–2690.
(105) Leforestier, C.; Szalewicz, K.; van der Avoird, A. Spectra of Water Dimer from a New Ab Initio Potential with Flexible Monomers. *J. Chem. Phys.* **2012**, *137* (1), 014305.
(106) Tschumper, G. S.; Leininger, M. L.; Hoffman, B. C.; Valeev, E. F.; Schaefer, H. F.; Quack, M. Anchoring the Water Dimer Potential Energy Surface with Explicitly Correlated Computations and Focal Point Analyses. *J. Chem. Phys.* **2002**, *116* (2), 690.
(107) Albertí, M.; Aguilar, A.; Bartolomei, M.; Cappelletti, D.; Laganà, A.; Lucas, J. M.; Pirani, F. A Study to Improve the van Der Waals Component of the Interaction in Water Clusters. *Phys. Scr.* **2008**, *78* (5), 058108.
(108) Buckingham, A. D. Permanent and Induced Molecular Moments and Long-Range Intermolecular Forces. In *Advances in Chemical Physics*; John Wiley & Sons, Inc.: Hoboken, NJ, USA, 1967; pp 107–142.
(109) Reimers, J. R.; Watts, R. O.; Klein, M. L. Intermolecular Potential Functions and the Properties of Water. *Chem. Phys.* **1982**, *64* (1), 95–114.
(110) Scribano, Y.; Leforestier, C. Contribution of Water Dimer Absorption to the Millimeter and Far Infrared Atmospheric Water Continuum. *J. Chem. Phys.* **2007**, *126* (23), 234301.

(111) Morawietz, T.; Sharma, V.; Behler, J. A Neural Network Potential-Energy Surface for the Water Dimer Based on Environment-Dependent Atomic Energies and Charges. *J. Chem. Phys.* **2012**, *136* (6), 064103.
(112) Matsuoka, O.; Clementi, E.; Yoshimine, M. CI Study of the Water Dimer Potential Surface. *J. Chem. Phys.* **1976**, *64* (4), 1351–1361.
(113) Lie, G. C.; Clementi, E.; Yoshimine, M. Study of the Structure of Molecular Complexes. XIII. Monte Carlo Simulation of Liquid Water with a Configuration Interaction Pair Potential. *J. Chem. Phys.* **1976**, *64* (6), 2314.
(114) Burnham, C. J.; Li, J.; Xantheas, S. S.; Leslie, M. The Parametrization of a Thole-Type All-Atom Polarizable Water Model from First Principles and Its Application to the Study of Water Clusters (N =2–21) and the Phonon Spectrum of Ice Ih. *J. Chem. Phys.* **1999**, *110* (9), 4566–4581.
(115) Fanourgakis, G. S.; Schenter, G. K.; Xantheas, S. S. A Quantitative Account of Quantum Effects in Liquid Water. *J. Chem. Phys.* **2006**, *125* (14), 141102.
(116) Paesani, F.; Iuchi, S.; Voth, G. A. Quantum Effects in Liquid Water from an Ab Initio - Based Polarizable Force Field. *J. Chem. Phys.* **2007**, *127* (7), 074506.
(117) Paesani, F.; Xantheas, S. S.; Voth, G. A. Infrared Spectroscopy and Hydrogen-Bond Dynamics of Liquid Water from Centroid Molecular Dynamics with an Ab Initio-Based Force Field. *J. Phys. Chem. B* **2009**, *113* (39), 13118–13130.
(118) Partridge, H.; Schwenke, D. W. The Determination of an Accurate Isotope Dependent Potential Energy Surface for Water from Extensive Ab Initio Calculations and Experimental Data. *J. Chem. Phys.* **1997**, *106* (11), 4618–4639.
(119) Ikawa, S.-I.; Maeda, S. Infrared Intensities of the Stretching and Librational Bands of H_2O, D_2O, and HDO in Solids. *Spectrochim. Acta Part A Mol. Spectrosc.* **1968**, *24* (5), 655–665.
(120) Fanourgakis, G. S.; Xantheas, S. S. The Bend Angle of Water in Ice Ih and Liquid Water: The Significance of Implementing the Nonlinear Monomer Dipole Moment Surface in Classical Interaction Potentials. *J. Chem. Phys.* **2006**, *124* (17), 174504.
(121) Babin, V.; Medders, G. R.; Paesani, F. Toward a Universal Water Model: First Principles Simulations from the Dimer to the Liquid Phase. *J. Phys. Chem. Lett.* **2012**, *3* (24), 3765–3769.
(122) Babin, V.; Leforestier, C.; Paesani, F. Development of a " First Principles " Water Potential with Flexible Monomers : Dimer Potential Energy Surface , VRT Spectrum , and Second Virial Coe Ffi Cient. *J. Chem. Theory Comput.* **2013**, *9*, 5395.
(123) Medders, G. R.; Babin, V.; Paesani, F. Development of a "First-Principles" Water Potential with Flexible Monomers. III. Liquid Phase Properties. *J. Chem. Theory Comput.* **2014**, *10* (8), 2906–2910.
(124) Góra, U.; Cencek, W.; Podeszwa, R.; van der Avoird, A.; Szalewicz, K. Predictions for Water Clusters from a First-Principles Two- and Three-Body Force Field. *J. Chem. Phys.* **2014**, *140* (19), 194101.